General Disclaimer

One or more of the Following Statements may affect this Document

- This document has been reproduced from the best copy furnished by the organizational source. It is being released in the interest of making available as much information as possible.

- This document may contain data, which exceeds the sheet parameters. It was furnished in this condition by the organizational source and is the best copy available.

- This document may contain tone-on-tone or color graphs, charts and/or pictures, which have been reproduced in black and white.

- This document is paginated as submitted by the original source.

- Portions of this document are not fully legible due to the historical nature of some of the material. However, it is the best reproduction available from the original submission.

Final Report

A FAST-NEUTRON SPECTROMETER OF ADVANCED DESIGN

Contract No. NAS8-11885
IITRI V6020-28
(formerly IITRI Project A6135)

to

National Aeronautics and Space Administration
George C. Marshall Space Flight Center
Huntsville, Alabama 35812

Attention: PR-RC

Final Report

A FAST-NEUTRON SPECTROMETER OF ADVANCED DESIGN

May 1, 1966, to June 30, 1967

Contract No. NAS8-11885
IITRI V6020-28
(formerly IITRI Project A6135)

Prepared by

W. E. Zagotta

and

R. B. Moler

of

IIT RESEARCH INSTITUTE
Technology Center
Chicago, Illinois 60616

for

National Aeronautics and Space Administration
George C. Marshall Space Flight Center
Huntsville, Alabama 35812

Attention: PR-RC

FOREWORD

This is the final report on IITRI Project V6020 (formerly A6135) entitled "A Fast-Neutron Spectrometer of Advanced Design," and covers the period May 1, 1966 through June 30, 1967. The work was performed for National Aeronautics and Space Administration under Contract No. NAS8-11885, Modification No. 5. The principal contributors to the research were R. B. Moler, C. C. Preston, and W. E. Zagotta.

Respectfully submitted,
IIT RESEARCH INSTITUTE

W. E. Zagotta
Research Physicist

R. B. Moler
Manager
Nuclear and Radiation Physics

Approved by:

F. L. Adelman
Assistant Director
Physics Research Division

/gjw

ABSTRACT

A FAST-NEUTRON SPECTROMETER OF ADVANCED DESIGN

This report describes the development and initial testing of a He^3 sandwich-type neutron spectrometer. The unique feature of this spectrometer is that the He^3 gas is used as the filling gas of two identical proportional counters. This feature permits effective discrimination against background gamma radiation, discrimination against interfering reactions in the silicon detectors, and an improvement in resolution, especially at low neutron energies.

The preprototype system exhibited a 5.48-MeV alpha resolution of from 150 to 250 keV, FWHM, and a thermal peak resolution of 200 keV. Testing with 2-MeV neutrons indicated that a peak was produced, but these tests were inconclusive because of the low flux and the presence of a large scattered component of the neutron flux.

It was found that, in the absence of a neutron source, no accidental gamma events could be observed up to gamma dose rates of 10^5 r/hr. However, with a neutron source present, high gamma backgrounds can cause pileup and can introduce accidental counts by causing an accidental coincidence between a solid-state detector and a true count in the two proportional counters. The pulse pileup reduces the energy resolution; at a gamma dose rate background of 300 r/hr, the alpha resolution was degraded to about 0.5 MeV. The accidental coincidences appear as a background which masks the thermal peak. No external shielding was used in these measurements.

A modification of the system to one using thinner solid-state detectors and a neutron converter material of Li^6 is suggested. It is expected that the modified system will perform in gamma backgrounds as high as 10^4 r/hr with a resolution of

about 0.5 MeV. A detailed design incorporating these and other changes intended to simplify the electronic circuitry is presented. Testing with this design is recommended.

A series of calculations of the energy- and angle-dependent efficiency of the He^3 system showed that the detector actually built has a highly anisotropic response, but that a similar spectrometer could be built which is fairly insensitive to the incident neutron direction.

TABLE OF CONTENTS

TABLE OF CONTENTS (Continued)

LIST OF FIGURES

I. INTRODUCTION

This report describes the progress made on a research program to develop a fast-neutron spectrometer and presents the results of a testing program on a preprototype system. The main objective was to design and develop a spectrometer capable of recording, with high resolution, spectra of the neutrons leaking through a liquid hydrogen tank on board a nuclear rocket propulsion vehicle. Such an instrument would also be useful for a wide variety of applications requiring neutron spectral measurements with good resolution and with good gamma rejection.

It is required that the spectrometer be capable of rapid measurements so that spectral changes could be determined while the liquid hydrogen is being depleted. It must also be capable of measuring neutron spectra in the presence of very high gamma fields. The specified environment was: fast neutron fluxes of 10^8 to 10^{10} neutrons/cm^2-sec, a maximum gamma field of 1.5×10^6 r/hr, and a time per measurement of 5 seconds. In addition to these environmental considerations, the resolution desired was 10 percent of the total reaction energy ($E_n + Q$) for neutrons of any energy between 0.1 and 14 MeV.

Much of the effort on this program was expended in solving the numerous difficulties which arose in putting together the many components of this intricate system and in developing a working instrument. Alpha sources were employed in adjusting the system and in determining the energy resolution. A brief testing program was performed to verify the operation of the spectrometer for fast neutrons and for thermal neutrons. A Co^{60} gamma-ray source was used to study the changes in both the alpha-spectrum and the neutron-spectrum measurements due to high gamma dose rate fields. Finally, a series of calculations of the efficiency as a function of neutron energy and of angle of incidence were performed.

II. DESCRIPTION OF THE SPECTROMETER

A. The Detector

This spectrometer is basically a He^3 sandwich-type spectrometer having the unique feature that the He^3 converter gas is used as the filling gas of two identical proportional counters. This unique feature has three advantages. The major advantage is that the spectrometer has very good gamma rejection. This rejection is obtained by admitting only those counts which are in coincidence with both proportional counters, which are inherently insensitive to gammas. Another advantage is that, by using the converter material as a proportional-counter filling gas, the energy loss in the gas can be electronically added to the signal to obtain good resolution at low neutron energy. This is in contrast to many sandwich-type spectrometers, which suffer from poor resolution at low neutron energies (< 1 MeV) because of the energy loss of the reaction products in the converter material. The third advantage is that the proportional counters can be used as dE/dx detectors, making possible particle recognition for the particles which completely traverse the active volume. In this way, the undesired (n,α) and (n,p) reactions in the silicon surface barrier detectors and the $He^3(n,d)D$ reaction can be eliminated. Otherwise, these reactions would lead to ambiguous spectrum measurements for neutron energies greater than about 4 MeV. These advantages are discussed in greater detail in a previous report,[1] which describes the development of an earlier version of this spectrometer.

B. The Block Diagram

The major difference between the earlier system and the present one is the incorporation of fast linear gates in the solid-state-detector signal path. The linear gates were incorporated to suppress the pulse pileup observed when the ungated system was exposed to high gamma fields. These gates are opened by the occurrence of a coincidence between pulses from the proportional counters. Such a coincidence occurs when a $He^3(n,p)T$ reaction takes place and the two emergent particles trigger the two proportional counters. In this way, gamma events in the solid-state detectors are prevented from reaching the main amplifiers. The main amplifiers should encounter, therefore, much lower count rates than the preamplifiers. This modification removes much of the pulse pileup which was observed in the main amplifiers in the older system.

A schematic diagram of the electronic components of the He^3 sandwich spectrometer is shown in Figure 1. The circuit is conveniently discussed in two parts: (1) the linear signals, and (2) the logic signals.

1. Linear Signals

The pulse from each solid-state detector, after being amplified in the preamplifier, passes through a long delay line. Because the solid-state detectors are inherently faster than the proportional counters, this delay line is inserted and adjusted to provide the proper timing to the logic circuits for the pulses from these two types of detectors. The linear signal emerging from the long delay line is attenuated to avoid overloading the linear gate, and then passed through another delay line. This short delay line delays the linear signal long enough so that the logic signal can pass through the logic circuitry and open the linear gate before the arrival of the

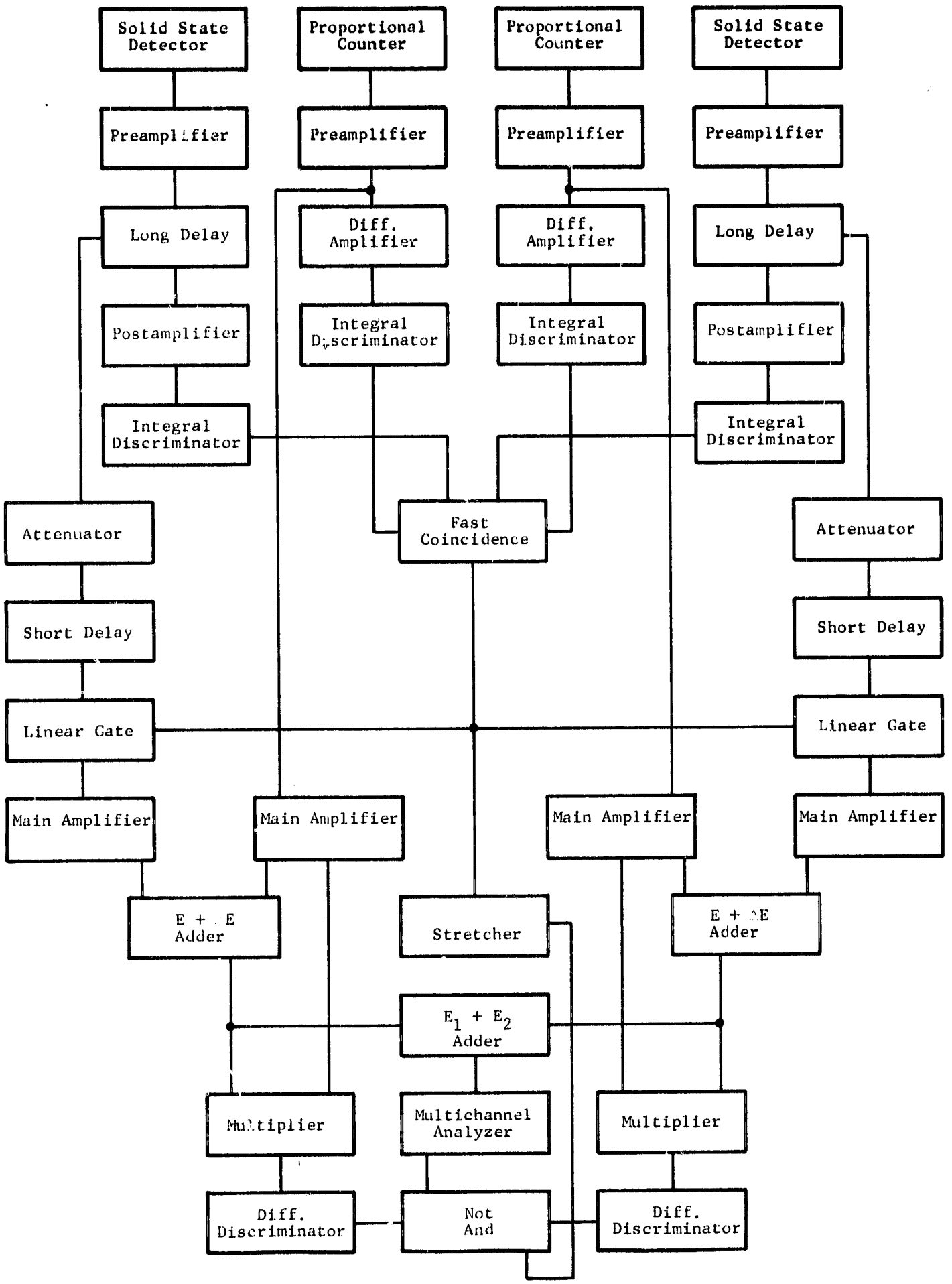

Figure 1 BLOCK DIAGRAM OF THE He^3 SPECTROMETER SYSTEM

linear signal. Since most of the pulses emerging from the solid-state detectors are gamma-induced or are due to other undesired events, the linear gate rejects a large fraction of the pulses arising from the solid-state detector. In this way, the slower components in the circuit, i.e., the main amplifiers, the adders, and the multichannel analyzer, are protected from pulse pileup. All of the circuitry before the gates is designed to be very fast and thus is less subject to pileup effects.

Those signals from the solid-state detector which pass the linear gates are introduced to the main amplifiers and then to the E + ΔE adders, where the signal representing the energy deposited in each of the proportional counters is electronically added to a similar signal from the corresponding solid-state detector. In this way, the degradation in resolution due to the energy lost in the He^3 gas is reduced. Before arriving at an adder, the linear signals from a proportional counter are amplified in a preamplifier and in a main amplifier.

After the corresponding solid-state-detector and proportional-counter signals are summed in the two E + ΔE adders, the outputs of these adders are summed in the $E_1 + E_2$ adder. The output of the $E_1 + E_2$ adder is then proportional to the total energy deposited in the four detectors enclosed in the chamber. This output is fed into the multichannel analyzer.

2. Logic Signals

There are two logic circuits in the system. The first circuit generates the pulses which open the linear gates. The purpose of this circuit is to reject all gamma-induced events and all neutron-induced events, the products of which do not deposit energy in all four detectors. The second logic circuit generates the pulses which open the analyzer. This circuit

rejects signals from the multichannel analyzer if they are due to interfering reactions in the silicon or He^3, or if they are due to $He^3(n,p)T$ events in which one of the reaction products escapes the active volume of the chamber.

The logic circuit which opens the linear gate will be discussed first. The logic signal from each solid-state detector is obtained from the linear signal after the long delay line. It is passed through an amplifier, called the postamplifier, to ensure that it will trigger the integral discriminator. The output of the integral discriminator goes to the fast-coincidence unit.

Thus, it is seen that there are four inputs to the fast-coincidence unit, one for each detector. An output is obtained only if these four signals are in coincidence. The output of the fast-coincidence unit is used to open the linear gates. In this way, gamma events are rejected because the Compton electrons cannot deposit enough energy in a proportional counter to trigger the corresponding integral discriminator. In addition, all neutron reactions which do not satisfy the fourfold coincidence condition are rejected.

The second logic circuit is a particle identification circuit. Particle identification is performed to eliminate the (n,α) and (n,p) reactions in the silicon and the (n,d) reaction in the He^3. These reactions lead to ambiguous pulse height distributions for neutron energies greater than about 4 MeV. Not all of these events are rejected by the fourfold coincidence condition.

The particle identification is accomplished by using the proportional counters as dE/dx detectors. In this discussion E' is the total energy of the particle, ΔE is the energy loss in the proportional counter, and E is the energy loss in the solid-state detector. The value of the product $E' \times \Delta E$ is approximately independent of energy for a given particle and

depends largely on the charge and the mass of the particle. The output of the E + ΔE adders is proportional to E'. The output of each E + ΔE adder is electronically multiplied by the output of the corresponding proportional counter to form the product E' x ΔE. This product signal is given to the differential discriminator which is set to pass only pulses induced by protons. In this way (n,α) and (n,d) reactions are eliminated. An (n,p) reaction in the silicon may not be thereby eliminated because both differential discriminators could pass pulses due to the proton. In this case the silicon reaction is eliminated by including a "not and" logic unit which takes advantage of the fact that the $He^3(n,p)T$ reaction can cause only one pulse induced by a proton. The circuit is set up so that a pulse opens the multichannel analyzer if one, and only one, proton is identified and if a fourfold coincidence has occurred. The stretcher is required because the pulse characteristics (dc level, pulse width and height) from the fast-coincidence unit are not compatible with the "not and" logic unit.

In summary, it is seen that the linear signals from the solid-state detectors are presented to linear gates which are set to reject gamma-induced and other undesired events and thereby reduce pulse pileup in the slow electronic components. They are then added to their corresponding proportional-counter signals and these sums are added to obtain a pulse whose height is proportional to the total energy deposited in the active volume of the chamber. The signal is presented for recording in the multichannel analyzer if one, and only one, proton was recognized, and if all four detectors were in coincidence.

C. Description of the Components

A detailed description of each electronic component is provided below. No attempt is made to describe the circuitry of the commercially supplied equipment, as this information can be readily obtained knowing the manufacturer's name and the model number, which are given when appropriate.

1. Detector Chamber

The detector chamber is shown schematically in Figure 2. The chamber contains two silicon surface barrier detectors separated by 2.6 cm. The active area is about the same as the area of the solid-state detectors, 2.00 cm^2. The intervening volume is equally divided by a series of seven 0.003-in.-diameter stainless steel wires, which form a virtual wall that electrically separates the two volumes. These wires are at chamber potential. The stainless steel wires of 0.001-in.-diameter, one in each volume and insulated from the chamber, are the anodes of each proportional counter. Small glass-to-metal seals (type 105-HT, Fusite Corp.) are used at one end of the wire, while miniature hermetic coaxial connectors (Microdot Corp.) are used at the opposite end. The solid-state detectors are mounted in the ends of the chamber with a hermetic coaxial feed-through connector (type C-14, Oak Ridge Technical Enterprises).

The chamber is generally filled with 0.25 to 0.50 atm of a gas mixture containing 87-percent He^3, 10-percent isobutane, and 3-percent argon. The high voltage used varies from 700 to 1400 volts.

2. Solid-State Detectors

The solid-state detectors used in this system are fully depleted silicon surface barrier detectors of 2.00-cm^2 area, 1100-micron depletion depth, and 29,000-ohm-cm resistivity. The detectors were manufactured by Ortec, Model SBCJ 200-1100.

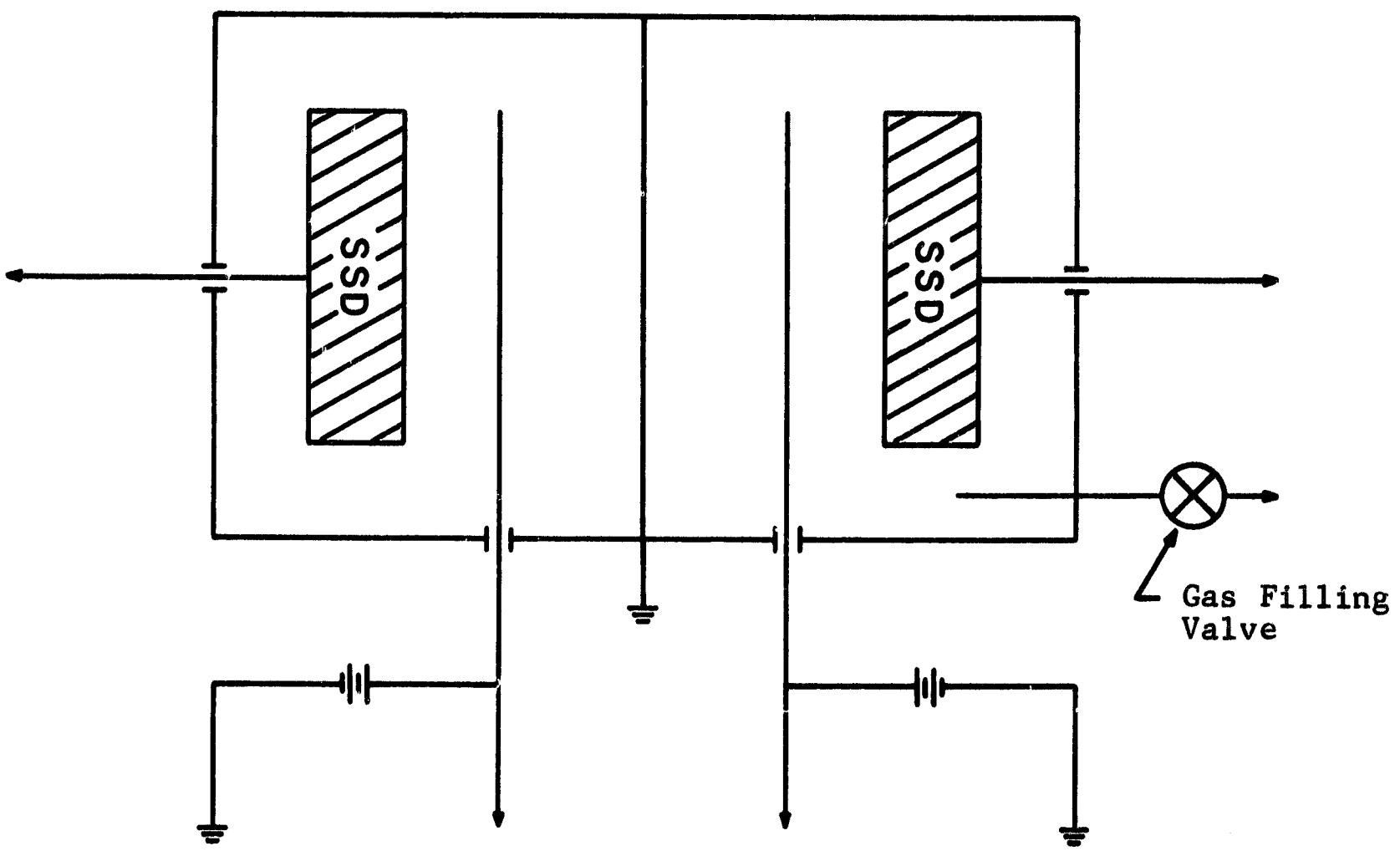

Figure 2 SCHEMATIC DIAGRAM OF THE He^3 SANDWICH DETECTOR

3. Solid-State-Detector Preamplifiers

To obtain the necessary fast pulses through the linear gate, a low-noise current-sensitive preamplifier having a rise-time of less than 25 nsec was desired. A low-noise preamplifier meeting these requirements was not available. However, it appeared that commercial charge-sensitive amplifiers (Tennelec 100B) could be modified to achieve the desired results. Consequently, the modification was accomplished by making the capacitive feedback loop resistive and reducing it to decrease the input impedence to about 100 ohms. Several other stabilizing networks were removed to increase the bandwidth. The modified preamplifiers have a rise-time of 40 nsec, which, while somewhat slow, is still adequate for our purposes at gamma dose rates less than 100 r/hr.

To measure neutron spectra in the presence of gamma dose rates higher than 100 r/hr, smaller pulse widths are required. At the time the dose rate problem was under study, the Solid State Radiations Inc., Model 112 current-sensitive preamplifiers became available to the project. These preamplifiers have less than a 3-nsec rise-time and a current gain of 300 (minimum). The output pulse width when connected to the solid-state detectors is about 50 nsec. For 5.5-MeV alphas, the peak height is about 40 mV. The noise (keV-FWHM) is quoted by the manufacturer as being ten times the total carrier collection time in nanoseconds, τ_c. Measurements indicate that better noise characteristics were actually observed. A resolution of about 200 keV was observed for τ_c = 50 nsec.

4. Proportional-Counter Preamplifiers

The preamplifiers for the proportional counters were designed and constructed to meet several constraints. Firstly, they should be low-noise charge-sensitive types; secondly, they

should have rise-times of 25 nsec or less; and, finally, they should be of solid-state design to facilitate repackaging for minimum size.

The circuit design chosen is a standard voltage-sensitive cascade, with direct coupling from the output emitter follower to the source of the input field-effect transistor. Voltage gain is 25, rise-time is better than 25 nsec, and the noise is approximately 100-μV-equivalent input signal.

5. Proportional-Counter Differentiating Amplifiers

A fast signal was required from the proportional-counter preamplifier to operate the fast proportional-counter integral discriminators. This is achieved by differentiating the output signal from the preamplifier. Since further amplification is required, both the differentiation and the amplification are performed with a differentiating operational amplifier. The gain of differentiated signal is about ten. The rise-time of this circuit is about 15 nsec.

6. Integral Discriminators

The four integral discriminators used in the system were manufactured by LeCroy Research Systems Corp., Model 121. This model provides continuously adjustable output pulse widths from 6 to 150 nsec. The threshold level of this instrument is fixed, and was measured to be about 0.070 V. The proportional-counter integral discriminators are set at 150-nsec output pulse width. The solid-state-detector integral discriminators are set at 6-nsec output pulse width.

7. Postamplifiers

The postamplifiers, needed for the additional amplification required to allow small signals to trigger the integral discriminators, are based on field-effect transistors. This is done to minimize loading of the circuit and to simplify the design. The circuit is a single voltage-sensitive feedback amplifier having a gain of 10 and a rise-time of less than 30 nsec. The stability, noise, and reliability of this circuit proved to be more than adequate for the purpose.

8. Fast-Coincidence Unit

The fast-coincidence unit was manufactured by LeCroy Research Systems Corp., Model 125. This unit has a front panel switch which selects the number of simultaneous negative signals required to generate an output pulse, with a maximum of four. The output pulse width may be continuously preset from 6 to 5000 nsec.

9. Linear Gate

The linear gate used in this system is the LeCroy Research Systems Corp., Model 124, Dual Gated Pulse Stretcher. As the manufacturer's name implies, in addition to gating the output, it generates an amplified and stretched pulse. The output pulse is +10 V maximum, with 100-nsec rise-time and a switch-selected fall-time of either 1 or 3 μsec. The high gain of these units removes the need for further amplification of the solid-state detectors. Thus, in Figure 1, the blocks labeled "Linear Gate" and "Main Amplifier" for the solid-state-detector lines are actually combined in a single module, the "Gated Pulse Stretcher."

10. Proportional-Counter Main Amplifiers

The main amplifiers used for the proportional-counter linear signals are manufactured by Tennelac, Model TC200. This versatile instrument provides a gain which can be varied from 4 to 2048, it features low-noise ($\leq$ 0.15 mV at all gain settings), variable rise-times, very flexible pulse shaping, and has no restriction on count rate.

11. Adders

The adders are based on a circuit reported by Rogers,[2] which was modified to provide somewhat faster rise-times and has the ability to pass positive signals linearly up to 10 volts.

12. Multipliers

The multipliers are based on the use of a differential pair of field-effect transistors, in which one signal is applied to the gates in series and the second is applied to the sources in parallel. The output taken from the drains is proportional to the product of the two signals over a reasonable range of signal sizes.

13. "Not And" Logic

The function of the "not and" logic is self-explanatory. It was constructed using standard integrated circuit "and" logic. This circuitry is all direct-coupled and has a minimum switching time of about 25 nsec. The logic output, which is required to open the linear gate of the multichannel analyzer, switches from "0" = -4 V to "1" = +0.5 V, and has a pulse width which is variable from 2 to 15 μsec.

14. Differential Discriminators

The differential discriminators are the Oak Ridge Technical Enterprises Corporation, Model 420 Timing Single Channel Analyzer.

15. Multichannel Analyzer

The multichannel analyzer is a 512-channel unit manufactured by Nuclear Data, Series 130, modified to accept 0.0- to 10-V input. Numerous equivalent systems could have served the same purpose.

III. EXPERIMENTS

A. Initial Adjustment and Operational Testing

Initially, a series of tests was performed using alpha-particle sources to adjust the various components and to aid in understanding the operation of the system. The adjustments which were considered in these tests were: the high voltage applied to the proportional counters, the length of the delay lines, the gain and pulse shape of the main amplifiers, the pulse width of the discriminators, the width of the fast-coincidence-unit output pulse (which is the same as the time the linear gate remains open), the adjustment of the $E + \Delta E$ adders, and the adjustment of the $E_1 + E_2$ adders.

An Am^{241} alpha source was used for these measurements. This source was prepared by evaporating a small spot of americium on each side of a strip of platinum. The platinum strip was then mounted on the wires which define the virtual wall of the two proportional counters. In this way, operation of each side of the chamber could be studied individually.

For this type of measurement the block diagram is considerably simplified, since the chamber is used one side at a time and since the particle identification circuit is not utilized (see Figure 3). The function of each block is the same as before, the important changes in the diagram being the following:

(1) The gates are opened by a coincidence between the solid-state detector and its corresponding proportional counter, i.e., a twofold coincidence;

(2) The variable attenuator present on the ΔE input from the proportional-counter main amplifier to the adder has been shown explicitly.

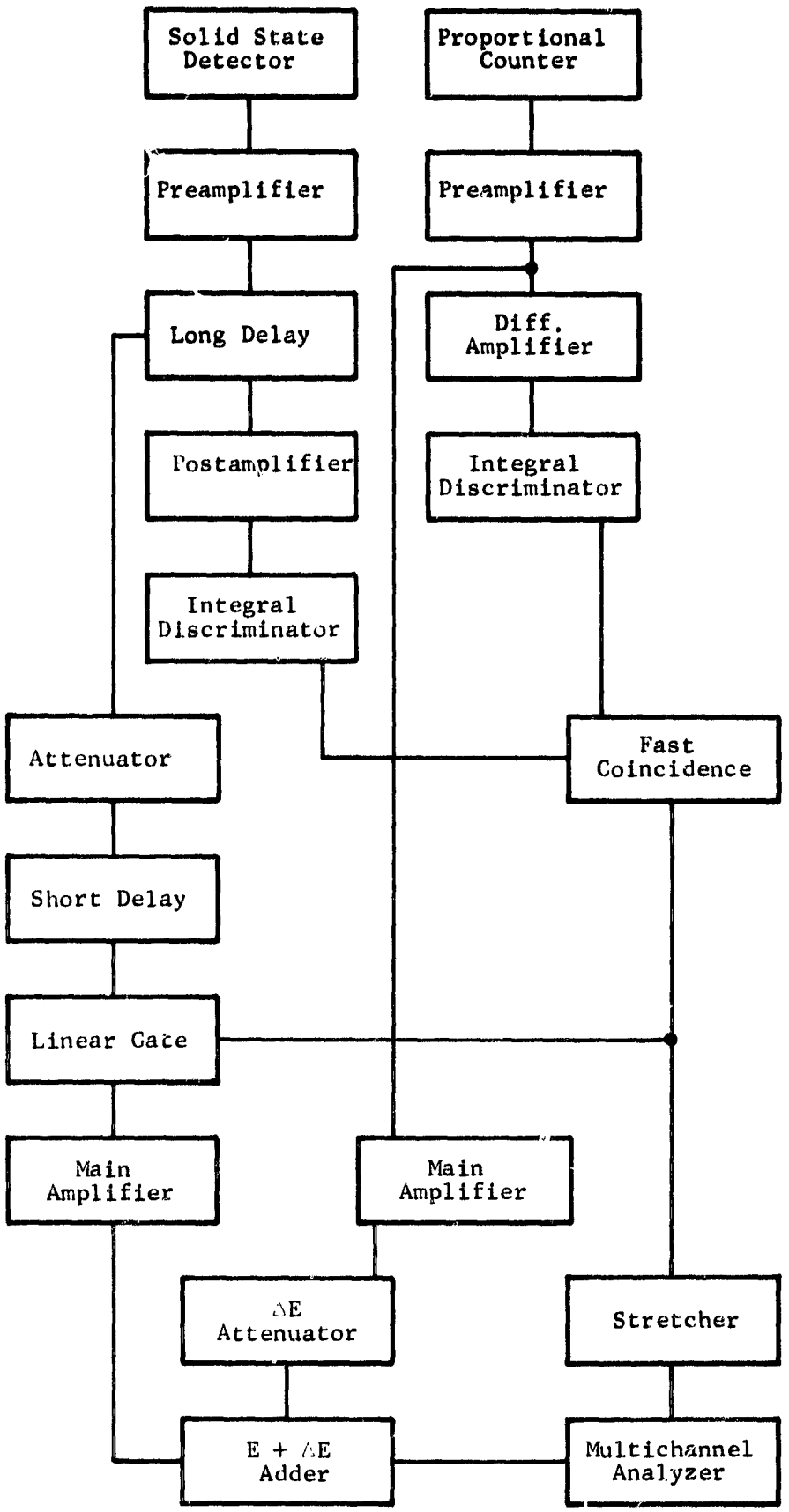

Figure 3 BLOCK DIAGRAM OF THE SYSTEM AS USED FOR TESTING WITH THE ALPHA SOURCE

This block diagram permits the counting of alphas. It is suitable for measurements even in high gamma fields, since a Compton-produced electron generally cannot deposit enough energy in a proportional counter to trigger the integral discriminator.

With this arrangement and with 100 feet of cable for the "Long Delay", the solid-state detector was brought into approximate coincidence with the proportional counter. However, they were not in perfect coincidence because of an effect which has been labeled as "jitter" in the proportional counter. Jitter occurs because charge produced far from the center wire takes a longer time to migrate than charge produced near the center wire. Another contribution to jitter occurs because of the 100-nsec rise-time of the signals coming from the proportional counters through the preamplifier and the differentiating amplifier; pulses of smaller amplitude take a longer time to trigger the discriminator than do larger pulses.

Both sources of jitter can be reduced somewhat by increasing the high voltage or by reducing the gas pressure. A 0.5-atm filling pressure with about 1000 volts on the anode was normally used. This value of high voltage was chosen because, at this gas pressure, it was about the highest that could be used without causing both breakdown problems and some anomalous behavior in the proportional counters; in particular, at higher voltages it appeared that counts in one proportional counter induced counts in the other proportional counter. Lowering the gas pressure reduced the breakdown voltage and therefore leads to similar problems if the voltage is unchanged.

This jitter is undesirable because it causes a degradation in resolution. In the original configuration the linear gate was triggered by the occurrence of a count in the proportional counter only. Because of the jitter, the gate would sometimes open before the arrival of the solid-state-detector signal, sometimes after this signal has passed, and

sometimes in-between these two extremes. Thus, the alpha peak was broadened because a variable fraction of the energy deposited in the solid-state detector was passed by the gate.

This difficulty was eliminated by using a twofold coincidence between the proportional counter and the solid-state detector. By using the minimum pulse width (6 nsec) for the logic pulse for the solid-state detector, only a 6-nsec jitter could occur between the arrival of linear signals from the solid-state detector and the opening of the gate. The short delay shown in the block diagram (about 10 nsec) ensured that the gate would always open before the linear signal arrived.

Because of the jitter, the number of twofold coincidences between the solid-state detector and the proportinal counter depends upon the width of the output pulse of the proportional-counter discriminator. For this reason the proportional-counter integral discriminator output was chosen to be 150 nsec, the widest possible with the equipment used.

After the initial determination of the best operating point for such parameters as high voltage and gas pressure, it is necessary to balance the system for the best resolution and for matched amplitudes in the two halves of the system. The first step in this procedure is to adjust the E + ΔE adders so that the energy lost in the gas by the alpha particle can be added to the solid-state-detector signal and thereby improve the resolution. For operational purposes, the optimum adjustment was defined to be that setting which yields the best resolution. The variation of resolution with ΔE attenuator adjustment for one typical case is shown in Figure 4. As seen from the figure, the resolution is improved by about 30 percent when the proportional-counter signals are included. The resolution for the optimum ΔE attenuator setting shown in the figure is about 250 keV, FWHM. With fresh gas filling, the resolution was frequently found to be as good as 150 keV.

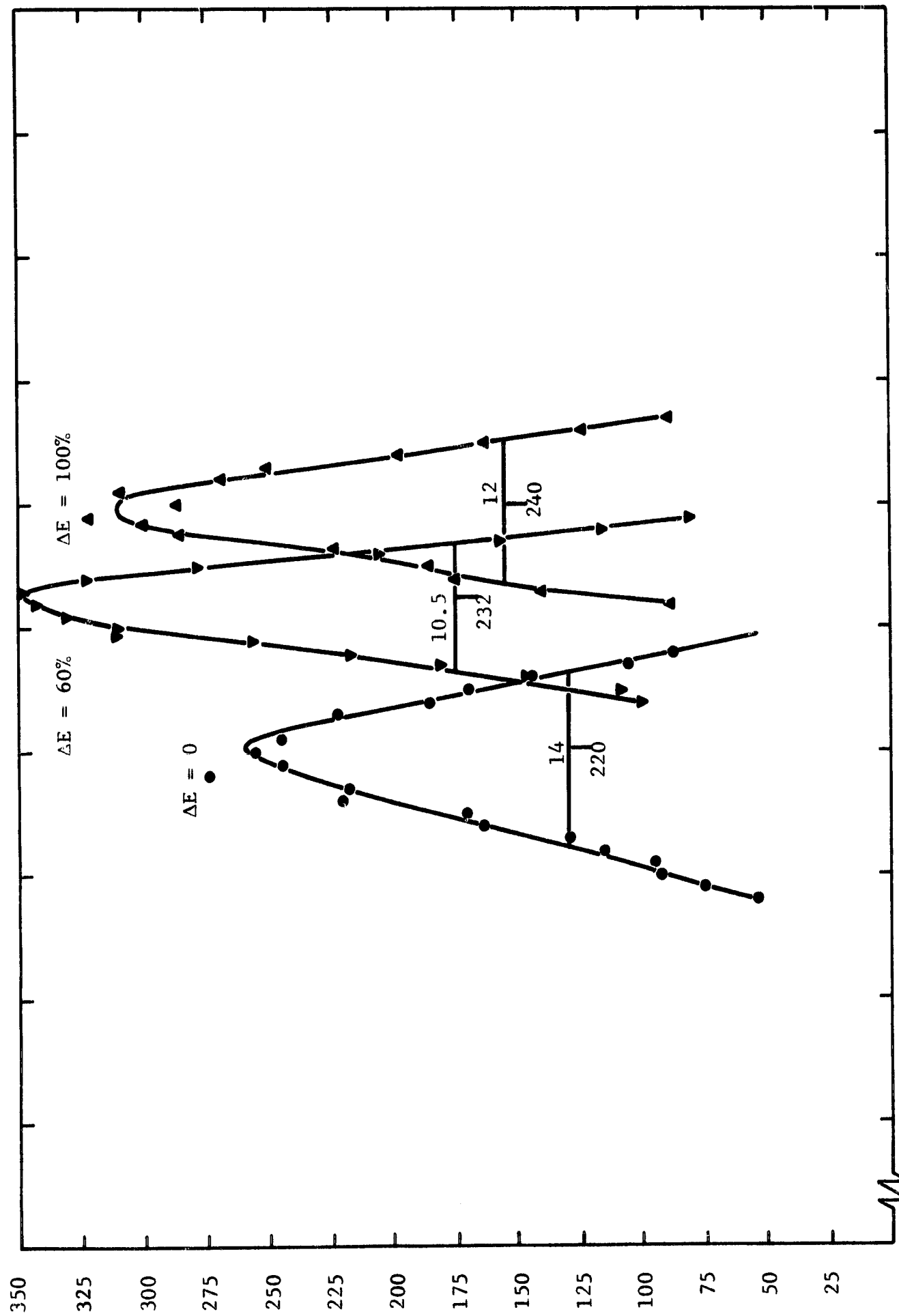

Figure 4 ALPHA PEAK AT VARIOUS ΔE ATTENUATOR SETTINGS

In general, after the E + ΔE adders are adjusted, the peak positions of the two sides are not identical. The $E_1 + E_2$ adder has a mixing adjustment which permits these peaks to be lined up. This ensures that the energy calibrations of both sides of the chamber are identical. To do this, the two sides of the spectrometer are both arranged as shown in the block diagram in Figure 3. Since there is only one fast-coincidence unit available, all four integral discriminators are connected to the fast-coincidence unit and the selector switch is set to give an output whenever a twofold coincidence occurs. This could result in the appearance of unwanted counts because the fast-coincidence unit could open the gates when, for example, two solid-state detectors are in coincidence. However, this occurs rarely because the only significant radiation sources present are the Am^{241} spots on the two sides of the platinum substrate. Since the alphas are emitted from independent sources, no true coincidence occur. Furthermore, this source is so small (0.1 curies) that the number of accidental coincidences is small. Thus, the vast majority of twofold coincidence occur between a proportional counter and its corresponding solid-state detector.

Each side of the spectrometer will present pulses at the $E_1 + E_2$ adder, but, in general, the pulses from side A will not be coincident with the pulses from side B. Thus, when the alpha spectrum is observed using the multichannel analyzer, two peaks appear near 5.48 MeV. By adjusting the mixing potentiometer, these peaks can be brought into alignment. When the two sides are almost aligned, the two peaks merge to form a single peak (sum peak). The width of the sum peak is an indicator of the alignment. The operational definition of optimum alignment is that the sum peak has minimum FWHM.

The system is completely balanced by this two-step procedure. No further adjustment of this balance is required if the adder inputs are not changed. However, it is found that the pedestal (base line) in the gated pulse stretcher drifts slightly during the course of a day or two. This must be checked periodically. This drift results in a shift of the zero of the energy scale up or down with fixed gain. For short runs, an hour or so, this drift is insignificant.

B. Performance Testing of the Spectrometer

1. Introduction

The objective of these tests was to determine the effect of gamma radiation upon the operation of the spectrometer. More specifically, it was intended to discover what effect gamma radiation had upon the shape of the spectrum and upon the resolution of the peaks.

Initially, a series of tests was performed with no external gamma sources present to determine the operation in this ideal case. Following this, a 500-curie Co^{60} source was used to study the changes in spectrometer behavior as a function of gamma dose rate. Cobalt-60 was chosen because its gamma-ray energy corresponds reasonably well to the average energy of the gammas emitted in the fission reaction (about 1 MeV).

2. Tests without Co^{60} Gamma Source

a. Tests with Alpha Sources

After the spectrometer-setup measurements were performed, the resolution of the 5.48-MeV Am^{241} alpha peak was measured. In the case where no Co^{60} source was present, this measurement was trivial, i.e., it was just the resolution obtained from the last of the setup measurements. The results of the measurements taken as the gamma dose rate was varied will be discussed in Section III B3a.

The alpha resolution of the balanced spectrometer in the absence of an external Co^{60} source was found to be in the range of 150 to 250 keV. The variation in observed alpha resolution results from the dependence of resolution on He^3 pressure and on the length of time since the chamber was cleaned and filled. This may indicate that the chamber leaked slowly or that the proportional-counter center wires became contaminated in some way which affected the resolution. It therefore became standard practice to clean the entire chamber periodically in an ultrasonic bath using acetic acid.

b. Thermal Neutron Tests

To remove the alpha counts from the neutron pulse height distributions, the fast-coincidence-unit selector switch is moved so that a threefold (instead of a twofold) coincidence is demanded between the proportional counters and one solid-state detector.

Originally, a fourfold coincidence was demanded for neutron spectrum measurements. However, it was found that the triton does not have enough energy to trigger the solid-state-detector integral discriminator. For this reason, all neutron pulse height distributions shown in this report were taken with only the threefold coincidence requirement. At thermal neutron energies the use of a threefold instead of fourfold coincidence still leads to unambiguous results at low gamma fields (< 10 r/hr). It may degrade the resolution somewhat because, for some events, the triton escapes the active volume of the chamber. This is not expected to be a large effect. In high gamma fields, the gammas which do appear when a threefold coincidence is employed are due to gamma interactions in the solid-state detectors. The threefold coincidence condition is met when a gamma interaction in a solid-state detector is in accidental coincidence with a PC-PC coincidence (a true neutron-induced coincidence between the two proportional counters).

Since only thermal neutron spectra were measured, there was no need for the particle identification circuitry, which is intended to remove the effect of interfering reactions. Such reactions tend to be important only above a neutron energy of 4 MeV.

Figure 5 presents the block diagram showing this somewhat simplified version of the spectrometer as it was actually used for all neutron pulse height distribution measurements.

Figure 6 shows a typical result of a measurement of the thermal neutron peak. The resolution of this peak is 190 keV, FWHM. During the course of these measurements the peak position was observed to drift as much as 10 or 15 channels (200 or 300 keV). It was found later that this peak drift was due to base-line drift in the Dual Gated Pulse Stretchers. The peak shown in this figure is at 0.55 MeV; the expected energy is the Q value of the He^3 (n,p)T reaction, 0.76 MeV.

Since this peak does not always appear at the expected position, further evidence was required to prove that the observed peak was in fact the thermal peak. Considerable uncertainty was felt on this point, especially before the Dual Gated Pulse Stretchers were found to drift.

It was shown that the peak intensity increased when the number of thermal neutron interactions in the detector increased, and that the peak resolution was about the expected value. These seemed to indicate that the peak was truly the thermal peak. On the other hand, the peak did not appear in the correct channel number.

The possibility that the peak could be due to gamma events following the absorption of thermal neutrons was considered. The arguments supporting this thesis were that it was capable of explaining the correlation of peak intensity with thermal neutron intensity and of explaining the incorrect energy of the peak channel.

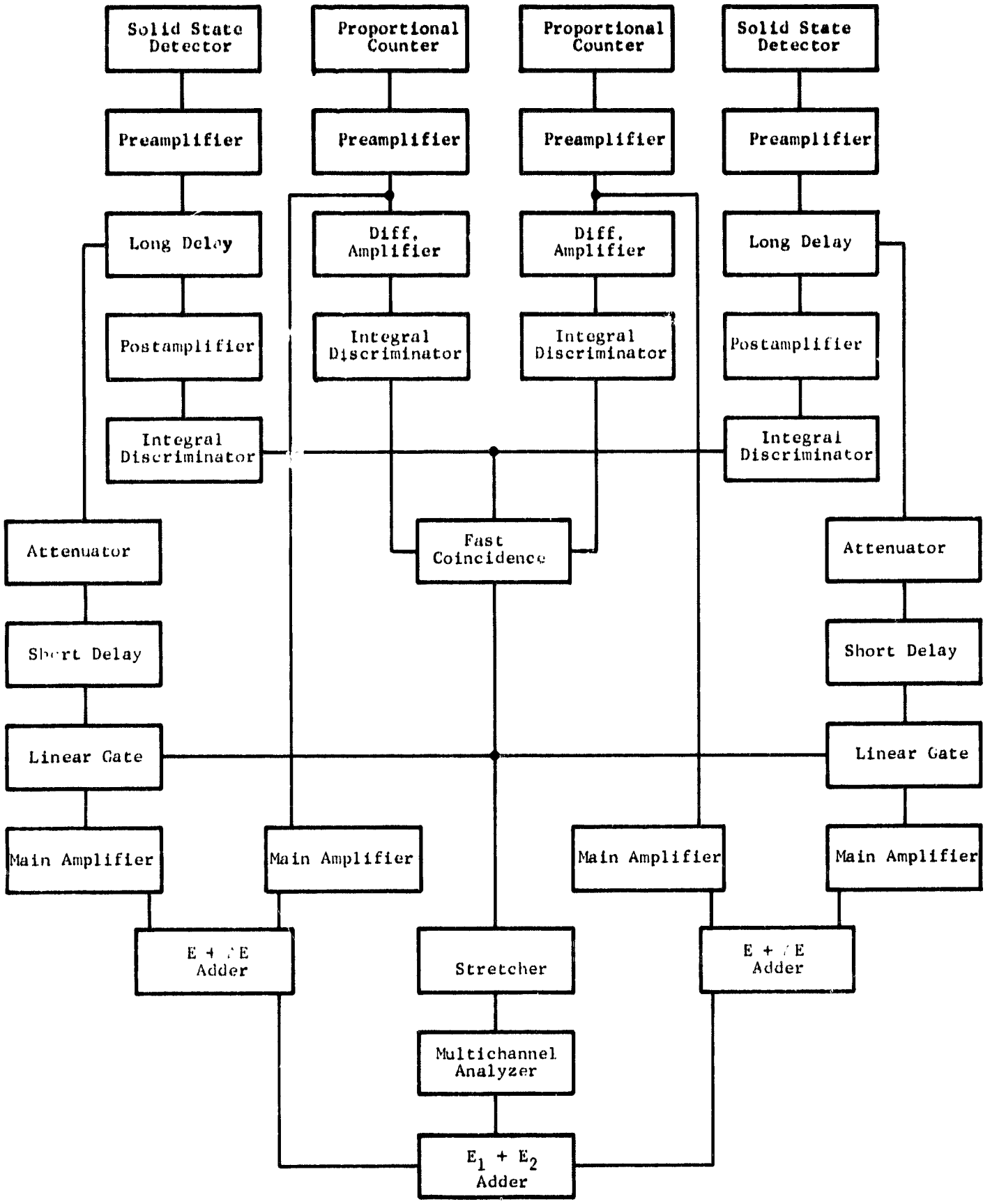

Figure 5 BLOCK DIAGRAM OF THE SYSTEM AS USED FOR TESTING WITH THE NEUTRON SOURCE

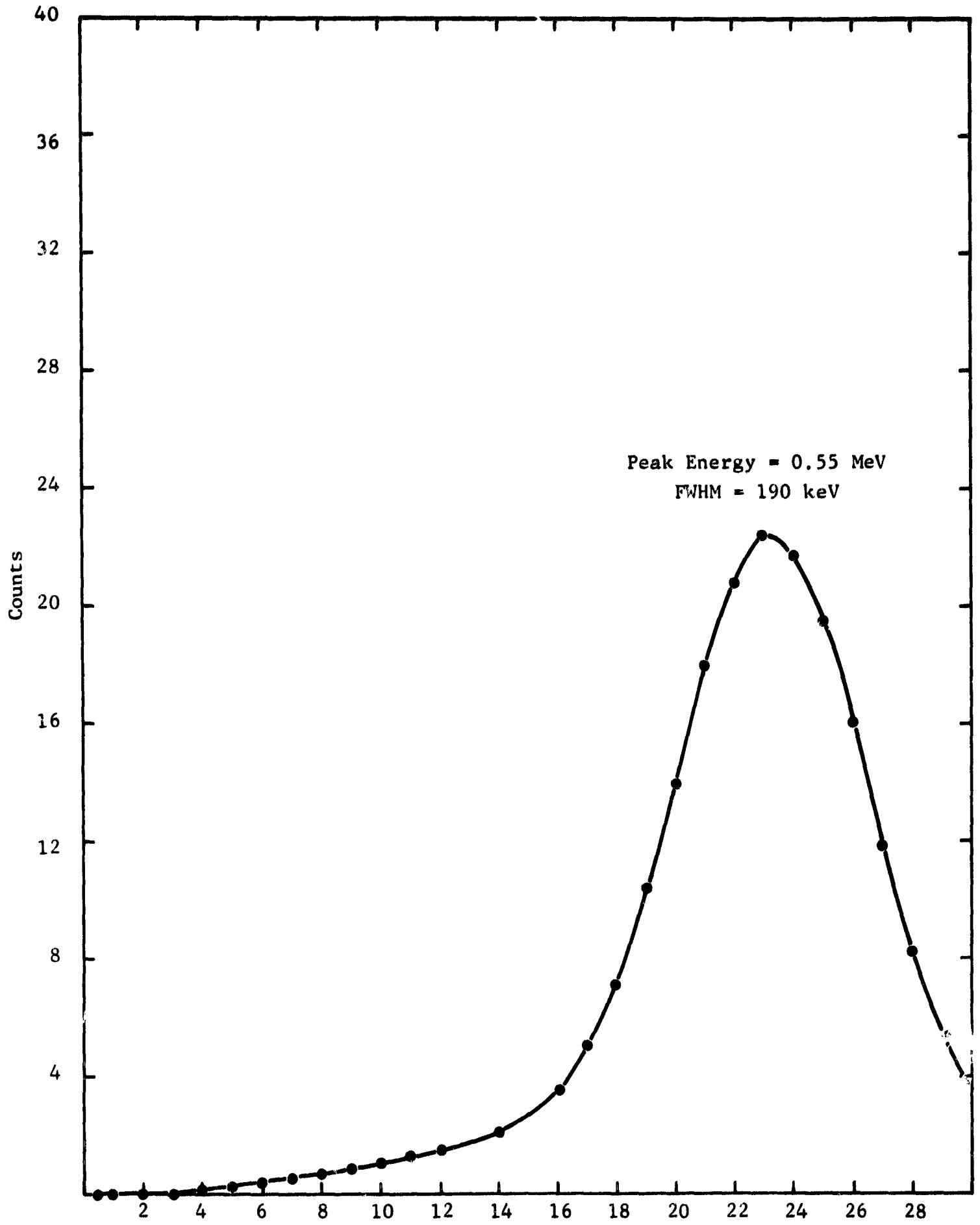

Figure 6 A TYPICAL THERMAL PEAK

If the peak were actually the thermal peak, it would have to be composed of two parts: the energy deposited by the proton in one solid-state detector and the energy deposited by the triton in the other solid-state detector. If the energy deposited by the proton and triton in the proportional counters is small, the output of each individual side of the chamber should show two peaks--one near 0.5 MeV due to those interactions where the proton is stopped, and one near 0.25 MeV from those interactions where the triton is stopped. When both sides are connected, the two peaks should produce a single peak at 0.76 MeV.

A low-energy neutron distribution was accumulated in which the output of only one side of the chamber was connected to the $E_1 + E_2$ adder to see if two peaks could be observed. (See Figure 7.) The peak near channel 21 is interpreted to be the proton peak. Because of baseline difficulties, the counts in the channels below channel 4 seem to be attenuated. The peak near channel 4 is interpreted to be the high-energy side of the triton peak.

The appearance of this structure in the low channel numbers is believed to be strong evidence that the peak in Figure 6 is indeed the thermal peak. This is better said in converse. When only one side is connected to the adders, a peak appears in channel 21 and a rise appears in a few of the lower channels. When both sides are connected, the peak appears in channel 23 and all the low-energy structure disappears. The disappearance of this low-energy structure and the slight upward shift of the peak position indicate that the peak in question is composed of two parts. This is believed to be good evidence that the thermal peak is actually seen.

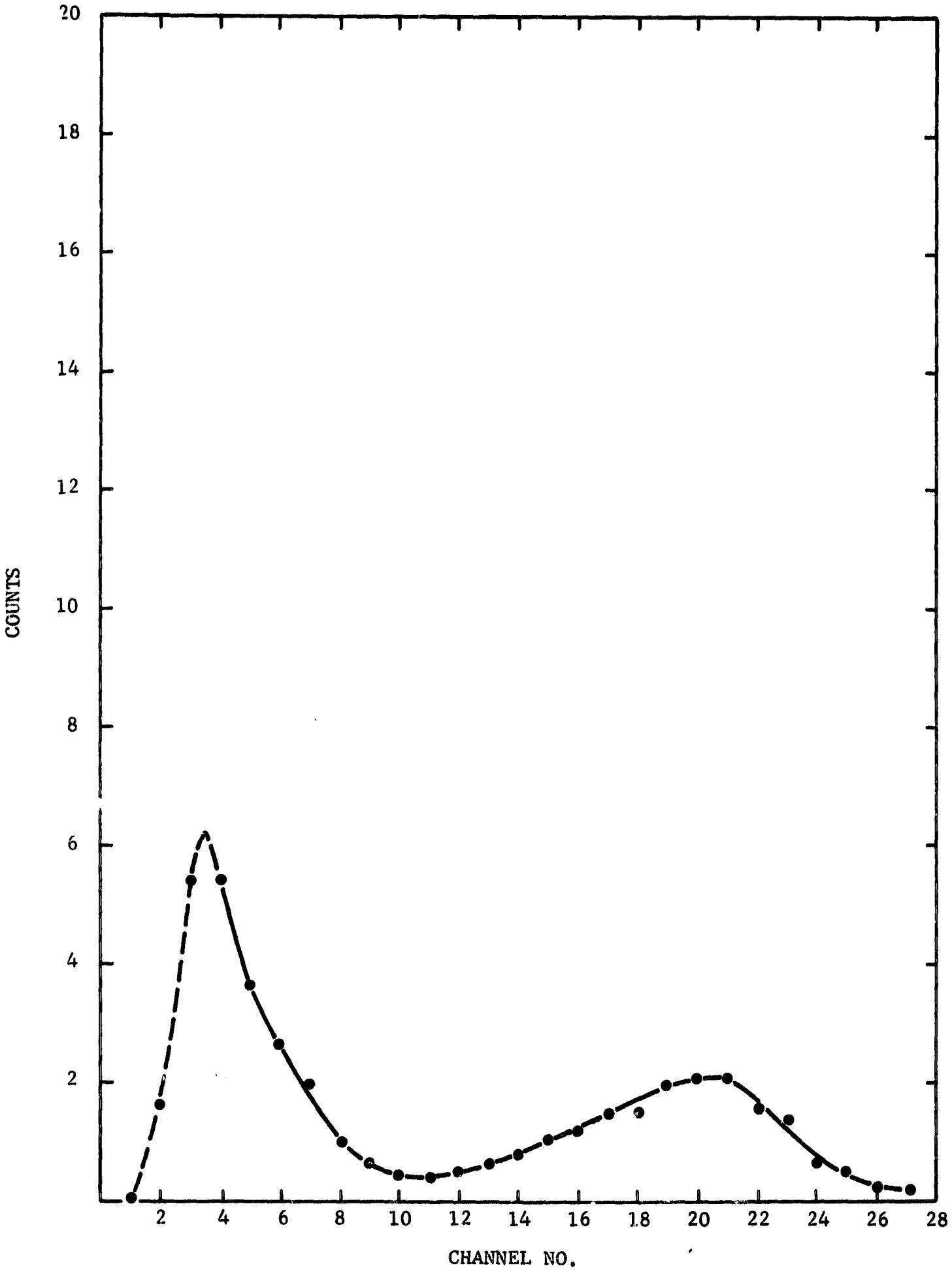

Figure 7 LOW-ENERGY DISTRIBUTION WITH ONE SIDE OF THE DETECTOR DISCONNECTED

c. Van de Graaff Tests

A brief series of irradiations was performed using the IITRI Van de Graaff. The neutrons were produced by bombarding a deuterium target with 1.5-MeV deuterons.

These measurements were seriously hampered by numerous extraneous circumstances which make the results difficult to interpret. The beam intensity was highly limited by operational constraints. A large scattering medium was present within inches of both the target and the detector. The target was opaque to deuterons, so that is was impossible to define the neutron energy uniquely.

The tests were intended to be only preliminary and were expected to show only that the spectrometer would respond to fast neutrons. Little effort was expended in trying to interpret the observed pulse height distributions. The criteria for deciding that the spectrometer was responsive to fast neutrons were (a) if a high-energy peak appeared when the spectrometer was exposed to neutrons from the $D(d,n)He^3$ reaction, and (b) if the peak shifted when the neutron energy was changed, then the spectrometer was working.

The test consisted of exposing the chamber to neutrons at two different angles, 160 degrees and 90 degrees, with respect to the beam direction. At 160 degrees and at 90 degrees, the neutron energy was expected to be about 2 MeV and 3 MeV, respectively. The only conclusive result of these tests was that, at 90 degrees, the high-energy limit of the measured pulse height distribution was greater than at 160 degrees. A peak was observed in the measurement at 160 degrees, but, at 90 degrees, the expected peak seemed to be smeared by the excessive background of scattered neutrons. Further testing on the Van de Graaff should be made.

The pulse height distribution measured at 160 degrees is presented in Figure 8. The steep slope below channel 20 is interpreted as gamma interactions in the solid-state detectors. The peak in channel 44 is the "thermal peak". This was verified by surrounding both the source and the detector with paraffin. The result exhibited no change in the high-energy part but exhibited a greatly enhanced peak in channel 44. The drop near channel 60 and the broad peak near channel 100 are believed to result from scattered neutrons entering the chamber. This scattering is from a medium composed primarily of SiO_2. The peak near channel 192 is believed to be due to the neutrons coming directly from the target. The energy corresponding to channel 192 is 1.5 MeV, which is somewhat lower than the expected value of about 2 MeV. The dotted line was obtained by taking the averages of four channels simultaneously.

3. Tests Employing a Co^{60} Gamma Source

The previous section described the performance of the spectrometer using radiation sources which were chosen specifically because the gamma radiation intensities are low. These tests were useful in studying the spectrometer performances; for example, the optimum delays and gain adjustments were decided upon, the alpha resolution of each side of the spectrometer was found to be between 150 and 250 keV, the thermal peak resolution was measured at 200 keV, and the spectrometer was shown to be responsive to fast neutrons in the 2-MeV range.

The tests described in this section were performed to study the effect of increasing the gamma dose rate in the experiments with the alpha source and with the ABC neutron source. These tests are considered to be the most important

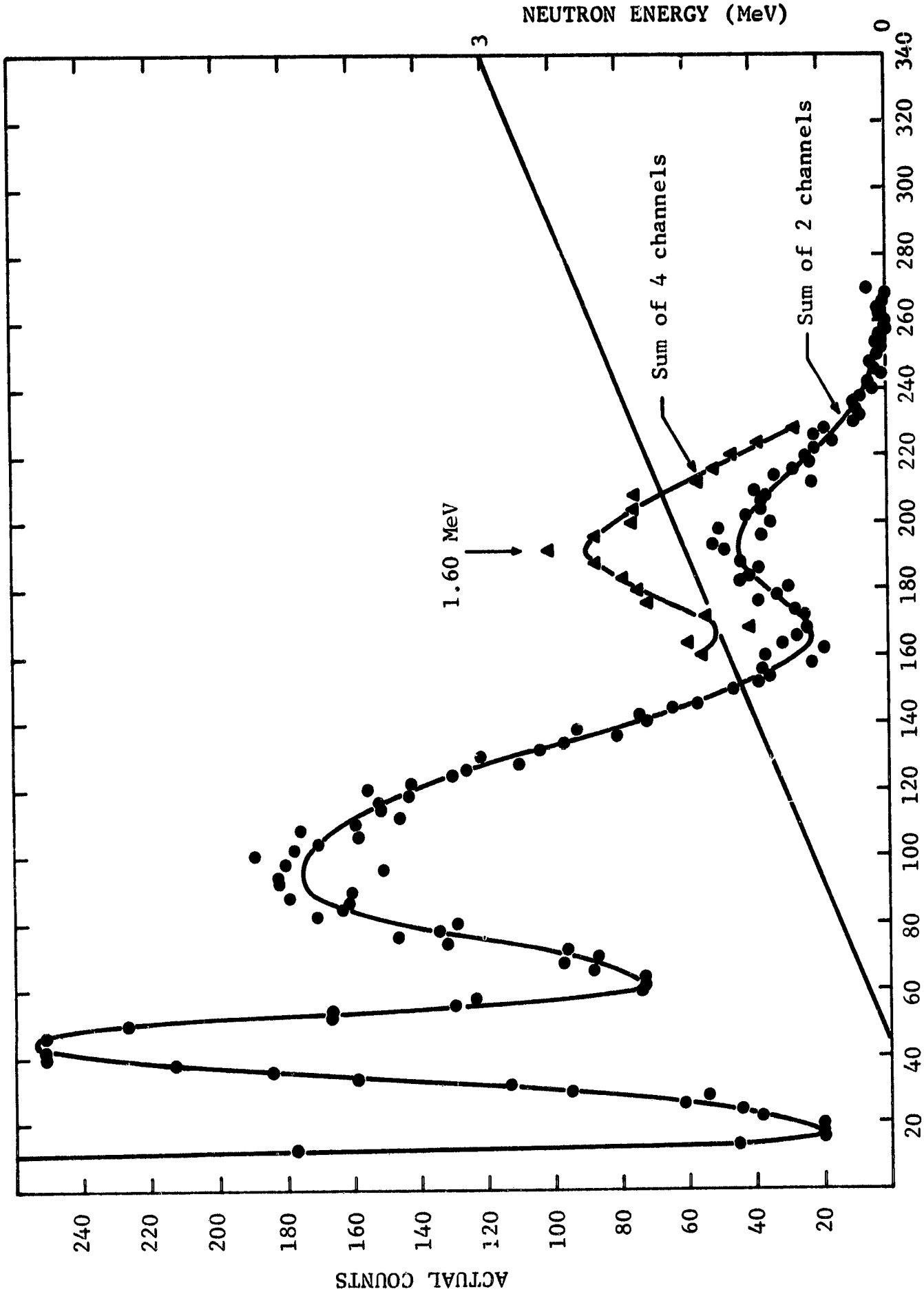

Figure 8 PULSE HEIGHT DISTRIBUTION USING THE (d,d) REACTION TO GENERATE FAST NEUTRONS

in the program. The desire to study the performance in high gamma fields was the main reason that the Van de Graaff measurements were terminated before more conclusive results were attained.

a. Tests with Alpha Sources

A 500-curie Co^{60} gamma-ray source was used to investigate the behavior of the spectrometer as a function of gamma dose rate. With this source, dose rates of the order of 10^5 r/hr could be obtained within a few inches of the source. These experiments were performed in a hot cell. The chamber and the preamplifiers were kept inside the hot cell to minimize the cable length between the detectors and their respective preamplifiers. All of the other electronics were outside the cell and thus protected from the high-radiation field. The system was set up as shown in the block diagram of Figure 3. The gate was 0.5 μsec when the slow preamplifier was used.

Figure 9 shows the effect upon the alpha peak of increasing the Co^{60} dose rate at the detector from 0 to 300 r/hr. Note the suppressed zero on the energy scale. At 0 r/hr the resolution is 270 keV, FWHM. As the dose rate is increased to 30 r/hr the resolution is essentially unchanged (300 keV), although the peak position shifts about 5 channels (140 keV). Note that the wings of the peak are increased somewhat, especially on the high side. When the dose rate is increased to 300 r/hr, the peak is broadened to 1.1 MeV, FWHM. Further peak shifting toward lower energies is obtained.

With 2 inches of lead shielding between the gamma source and the detector, the gamma dose rate was reduced by a factor of 10. The alpha peak position and FWHM at 300 r/hr with 2 inches of lead is seen to be the same as for 30 r/hr with no lead.

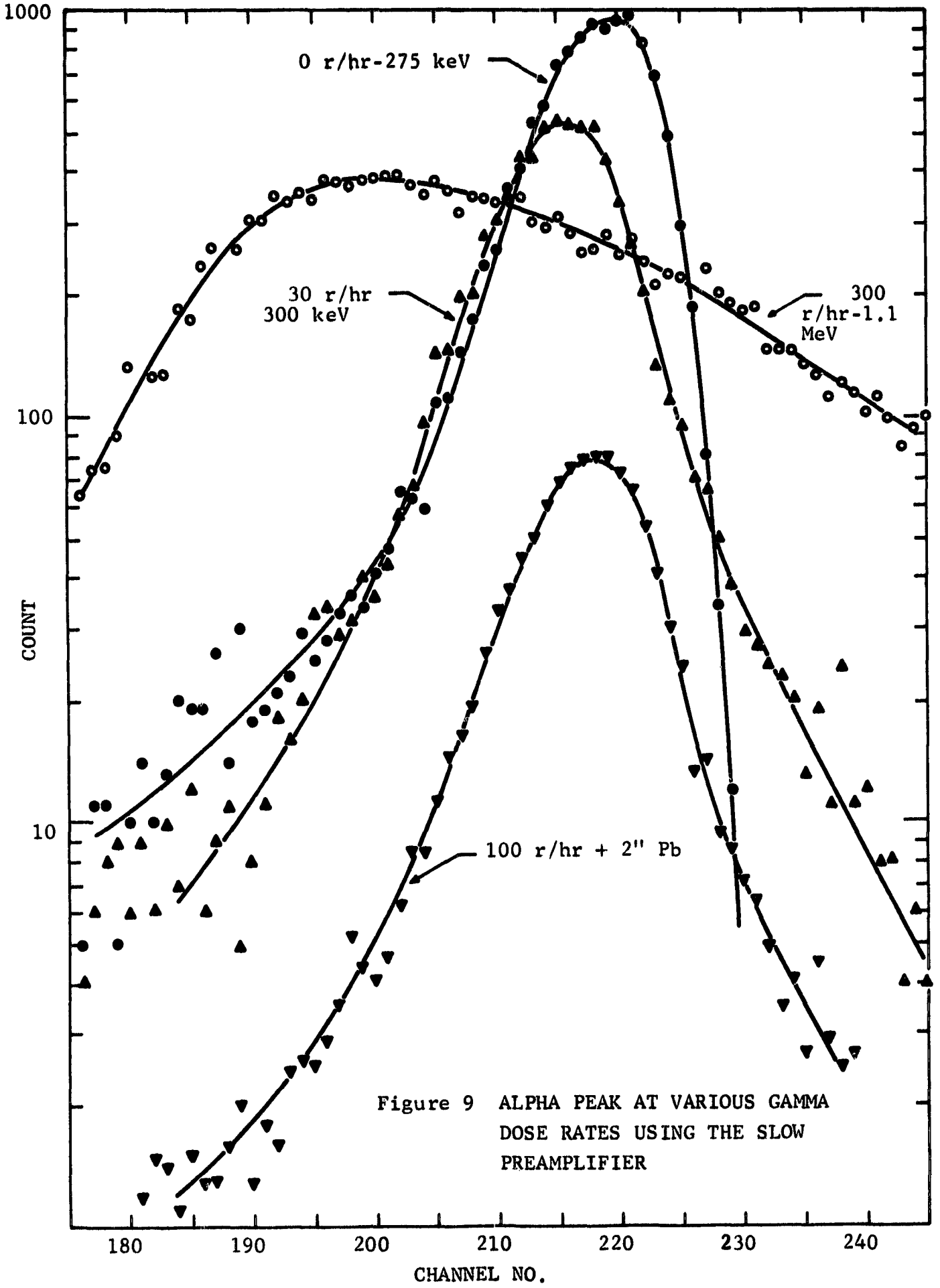

Figure 9 ALPHA PEAK AT VARIOUS GAMMA DOSE RATES USING THE SLOW PREAMPLIFIER

The peak spreading at 300 r/hr is believed to be due to the fact that, at high dose rates, a gamma ray interacts with the solid-state detector while the gates are opened to allow the passage of the alpha-particle energy deposited in the solid-state detector. In this way some fraction of the gamma-ray energy is added to the alpha-particle energy and thereby causes an upward shift in the peak position and a decrease in resolution. To test this conjecture, an order-of-magnitude quantitative estimate was performed, even though the hypothesis could not explain the direction of the energy shift.

For Co^{60} at 300 r/hr, the gamma-ray number flux is about 2×10^8 gamma-rays/cm^2-sec. If these are incident normal to a solid-state-detector surface, the number of gammas passing through the 2 cm^2 area of the detectors is 4×10^8 sec^{-1}. The thickness of these detectors is 0.11 cm. Since the mean free path for Co^{60} gammas in silicon is 6.7 cm, 0.11/6.7 = 0.016 is the fraction of the incident gammas which will interact. Thus, the gamma interaction rate is 0.66×10^7 interactions per second. On the average then, a gamma interaction will occur every 150 nsec. For these measurements the gate width was about 400 nsec. It is therefore almost inevitable that an alpha interaction will be accompanied by at least one gamma interaction. Since each gamma can deposit about 0.5 MeV in the solid-state detectors, theoretically a spread of about this energy can be expected. The observed spreading in Figure 9 is about 1 MeV. This is regarded as reasonably good agreement between experiment and this approximate theory. Thus, it is believed that the peak broadening is due to the gamma energy deposited in the solid-state detectors while the linear gates are opened by the occurrence of an alpha interaction. With this postulate a peak shift toward higher energy should also be observed as the dose rate is increased. However, the

peak is observed to shift toward lower energy. It is assumed that the upward peak shift is canceled by some other overriding effect. As yet, no definite mechanism for the downward shift has been identified. One conjecture is that the peak shift is due to a baseline shift in the solid-state-detector preamplifiers while operating at very high count rates.

It is clear that the degree of broadening is related directly to the number of gamma interactions occurring while the gate is open. If the gate is open for a shorter time, then fewer gamma interactions occur while the gate is open and the broadening is reduced. A faster preamplifier is required to get all of the charge, which is deposited in the solid-state detector, through the gate at shorter gate widths. The Solid State Radiation Inc. preamplifiers described in Section II C3 were employed to permit faster gating. The modified Tennelec 100B preamplifier, also described in Section II C3, has an output pulse width of about 150 nsec. Because this preamplifier exhibits some overshoot, a gate width of about 450 nsec was required. The Solid State Radiation Inc., Model 112 preamplifiers have an output pulse width of only 50 nsec with very little overshoot. All the charge was completely passed with a gate width of 100 nsec.

A series of spectra taken with the faster preamplifiers and with a 100-nsec gate width is shown in Figure 10. These curves are to be compared with Figure 9. It is seen that no broadening occurs up to about 30 r/hr (in fact, an experimentally insignificant improvement in the resolution was observed). At 300 r/hr the peak had begun to broaden. However, with the faster preamplifier the peak width is only about 20 channels (0.5 MeV), compared to the 45 channels observed at this dose rate with the slower preamplifiers.

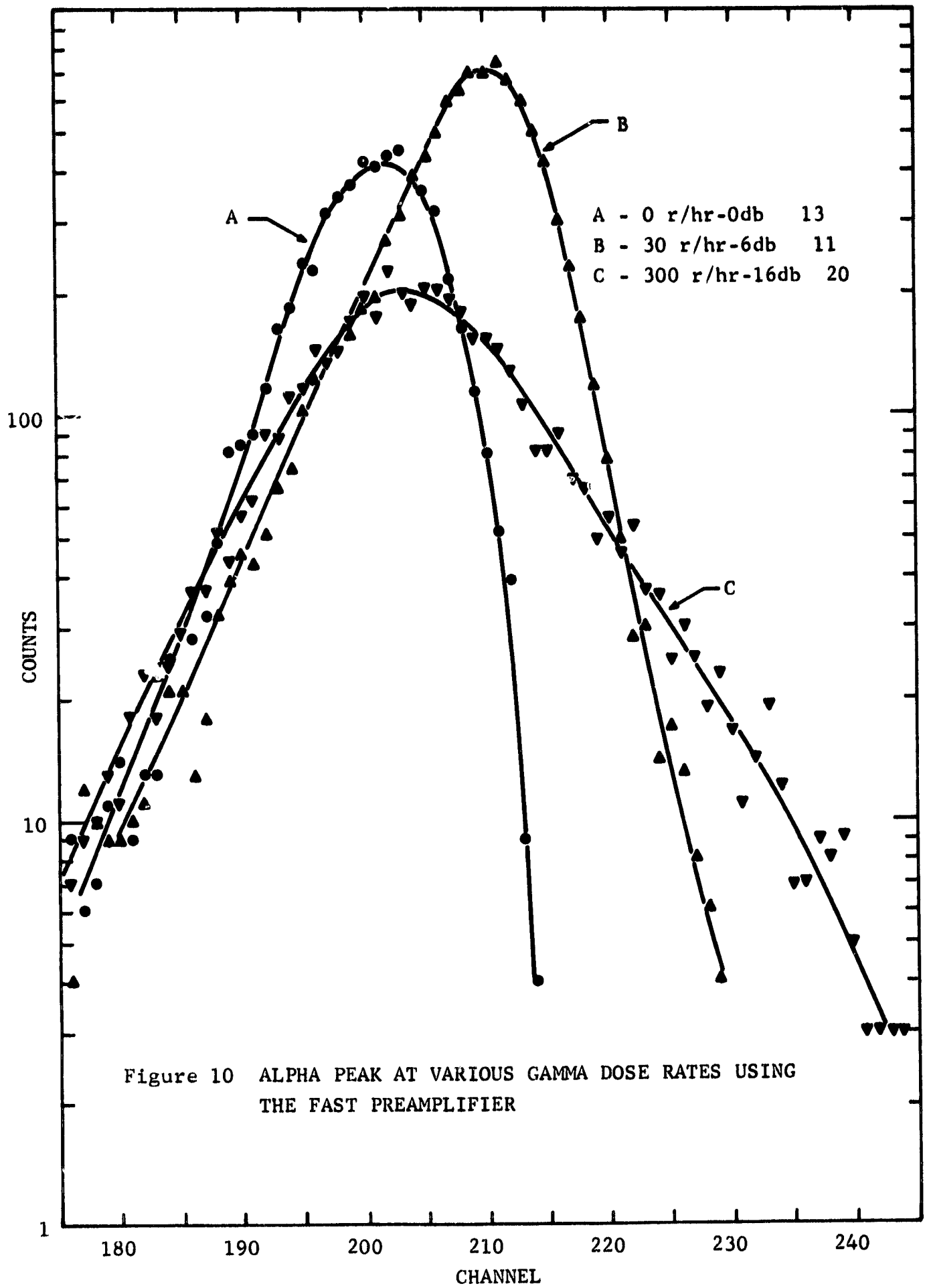

Figure 10 ALPHA PEAK AT VARIOUS GAMMA DOSE RATES USING THE FAST PREAMPLIFIER

The peak position is seen to shift when the gamma dose rate is increased. It is seen that, with this faster preamplifier, the peak shifted upward as the dose rate was increased to 30 r/hr, and reversed and shifted downward as the dose was increased to 300 r/hr. Note that the alpha peak shifting with the fast preamplifier (<8 channels) was much less than with the slow preamplifier (~20 channels).

(1) Modifications to Obtain Shorter Gate Widths

It is observed that the shorter gate width obtained by using faster preamplifiers on the solid-state detectors is effective in reducing the resolution broadening in the presence of high gamma fields. An even faster gate width can be achieved only if the gate linear input pulse is made faster. When the Model 112 preamplifiers are used, the speed of the input pulse is not controlled by the preamplifier but rather by the speed of the solid-state detector. The electron transit time for these 1100-micron detectors at room temperature is calculated to be about 60 nsec, which is close to the 50 nsec observed. Any further increase in speed will therefore have to be attained by shifting to faster solid-state detectors.

The speed of detectors can be increased in three ways: increase the bias voltage, decrease the detector thickness, or decrease the temperature. Only room-temperature operation will be considered. Normally, the solid-state detectors were operated with 150-V bias. This bias is close to the manufacturer's warranted bias voltage, 180 V. The detector thickness was chosen to be adequate for stopping 12.50-MeV protons. If the thickness were to be reduced, the upper energy limit of the spectrometer would also be reduced.

It appears, therefore, that there is no satisfactory way of increasing the speed of these pulses as long as the $He^3(n,p)T$ reaction is employed. However, if the $Li^6(n,\alpha)T$ reaction is utilized as the neutron converter, a significant improvement can be realized. Since the reaction products are heavier, they have shorter ranges, permiting thinner detectors to be employed. Thinner detectors, in turn, permit faster charge collection time and hence shorter gate widths.

For example, a 14-MeV neutron will generate a triton and an alpha. The detector thickness will be determined by the particle having the greater range, i.e., the triton. The triton range will be less than 200 microns in silicon. Oak Ridge Technical Enterprises Corporation supplies a 300-micron detector which yields a guaranteed alpha resolution of 40 keV and an electron transit time of 7 nsec (compared with the calculated value of 60 nsec for the 1100-micron solid-state detectors currently used). With such fast pulses the gate width is expected to be reduced from 100 nsec, which is the shortest used so far, to less than 20 nsec. This, in turn, will increase the gamma dose rate required to give the same gamma energy deposition during one gate opening. Since these are linear relationships, the gamma dose rate required to broaden the resolution to approximately 0.5 MeV is expected to increase by at least a factor of 5 (from 300 to 1500 r/hr)

due to the narrower pulse width (20 nsec instead of 100 nsec). In addition, the 300-micron detector will interact with fewer gammas. Since this is also a linear relationship, the maximum gamma dose rate is expected to increase to about 5500 r/hr when the detector thickness is reduced from 1100 to 300 microns. A further increase will result from the fact that, on the average, less gamma energy will be deposited in the thinner detectors; however, no quantitative estimate has been made of this effect.

At the present time all of the electronic components are capable of handling signals of this speed. At the present time the speed is limited by the solid-state detector. The problems associated with a switchover to the fast system are expected to be (a) termination and pulse shape considerations to remove reflected pulses and overshoot on the preamplifier output, and (b) introduction of the Li^6 into the system.

Some other significant advantages will be realized if a lithium converter is utilized. Fourfold coincidences should be achieved because the higher Q value of the reaction makes it easier for the reaction products to traverse the gas. Fourfold coincidences were never observed in the present system. Another significant advantage, which will be discussed in the next section, is that measurement of the thermal peak in high gamma fields will be made easier.

Once the speed of the system is increased, the spectrometer is expected to operate in fields of more than 5500 r/hr, compared to the current maximum of 300 r/hr. It is expected that the limitations of the faster system will be the result of two separate effects. The first is the peak shifting which was observed in the spectra shown in Figures 9 and 10. At the present time this peak shifting is unexplained. The second effect, which has not been observed as yet but is known to exist, is that the proportional-counter gain decreases as the

gamma dose rate increases. This is not an important effect at 300 r/hr. At 10^6 r/hr it is known to cause a large enough decrease in gain that the signal from the proportional counters is not great enough to trigger the integral discriminators; the entire spectrometer is then inoperative. It is not known how important the effect will be at, say, 10^4 r/hr. This effect has been studied by Spielberg,[3] who reports that the effect can be significantly reduced by using tungsten center wires instead of stainless steel and by utilizing larger center-wire diameters.

(2) Comparison of Techniques for Suppressing Gamma Events

These measurements in high gamma fields indicate the value of the gated system as a tool to permit gamma discrimination. At 300 r/hr, the rate of interactions in the solid-state detector is $> 10^6$ per sec. No multichannel analyzer currently in existence could handle such a count rate. The gated spectrometer, which eliminates the gamma counts through the use of the proportional counters, yielded count rates of < 300 counts/sec. This is well within the count rate capabilities of most analyzers.

Pulse shape discrimination is sometimes used to obtain gamma rejection. However, systems employing proportional counters and pulse shape discrimination have an inherently slow response and would be inoperative at count rates of 10^6 per second. While solid-state detector systems employing pulse shape discrimination have been developed recently, at 300 r/hr the count rates are already slightly beyond the current state of the art. At ten times this dose rate, pulse shape discrimination appears to be impossible.

Another alternative is to use external gamma shielding. While this alternative could be applied to any or all systems, it is believed preferable to push the state of the art as far as possible without shielding, in order to

minimize the weight requirements. Furthermore, external shielding materials might interfere with the neutron spectrum measurement.

b. Thermal Neutron Tests

A series of tests were performed with the ABC source to determine the effect of increasing the gamma dose rate on the thermal peak. The system was set up as shown in the block diagram of Figure 5 using the slow preamplifiers. The thermal peaks obtained in various gamma fields are shown in Figure 11. As the gamma dose rate is increased, a broad continuum appears under the peak and the peak shifts to a lower channel number. The first effect occurs because the high gamma-induced count rates in the solid-state detectors produce accidental coincidences with the thermal neutron-induced coincidences with the proportional counters. This effect is very similar to the effect which produced the alpha peak broadening in the alpha source tests.

The first effect, the appearance of the broad continuum under the thermal peak, arises because false counts can be passed by the logic when a gamma interaction in the solid-state detector occurs simultaneously with a neutron interaction in the proportional counters. It is noteworthy that both sources must be present for the broad continuum to appear. If the ABC source is removed and the gamma source remains, no counts are passed by the logic. This is important because it demonstrates that the proportional counters are behaving properly. No counts appear because the gamma-insensitive proportional counters are unable to generate accidental coincidences even in very high pure gamma fields. Therefore, the logic will not open the gates or the analyzer. However, with the ABC source present, the neutrons generate true coincidences between the proportional counters.

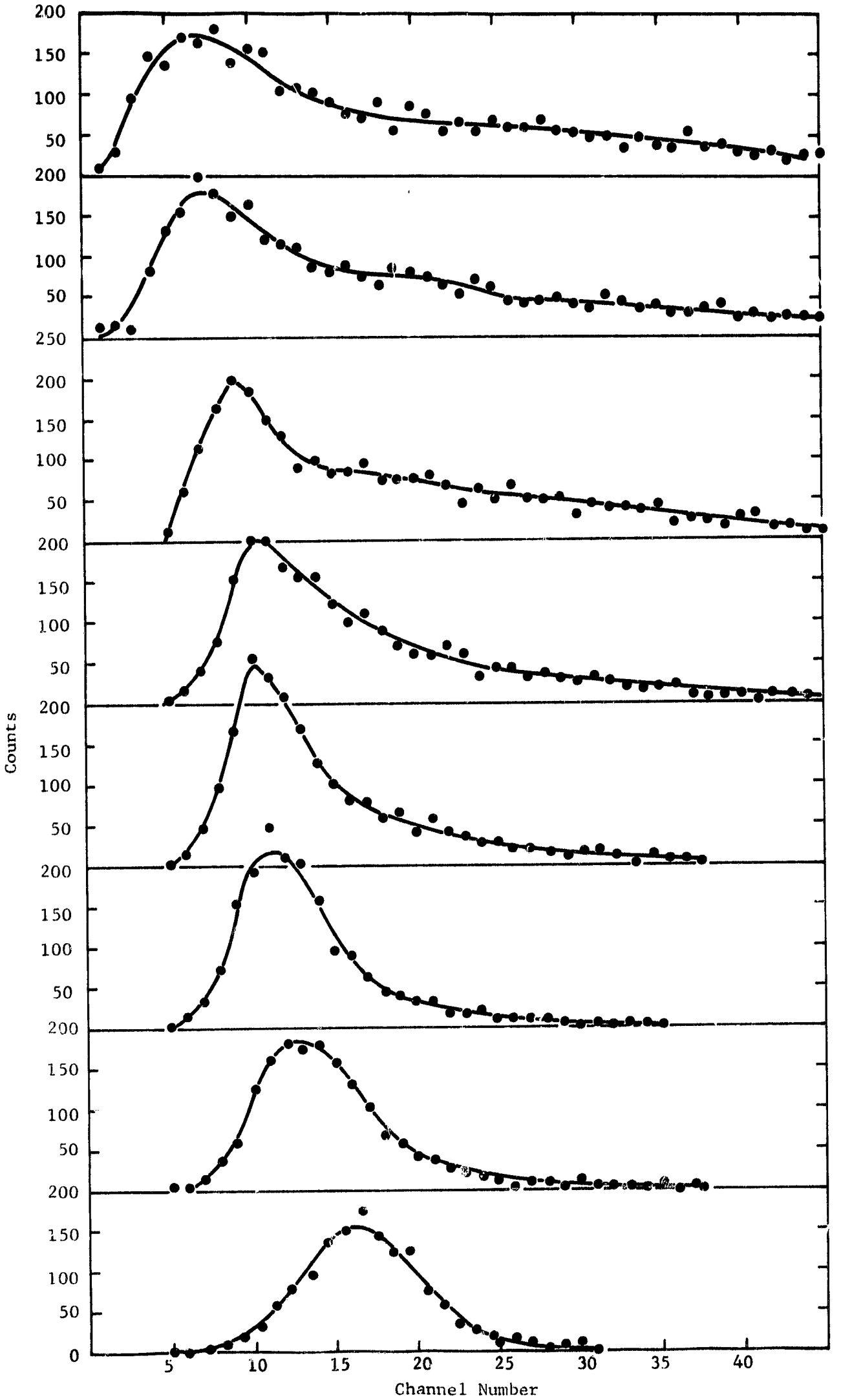

Figure 11 THERMAL PEAK AT VARIOUS GAMMA DOSE RATES

Two possibilities now exist: either the proton and/or triton will interact with a solid-state detector or it (they) will not. If neither particle interacts with the solid-state detector, the conditions for a threefold coincidence can still be met if a gamma interaction occurs simultaneously in the solid-state detector. Since a gamma can deposit any energy from zero to almost the full gamma energy, this case results in a broad continuum from zero to the full gamma energy. The second case, in which a true neutron-induced threefold coincidence occurs, would result in a thermal peak if no gammas were present. If a large number of gamma interactions are occurring in the solid-state detector, then this thermal peak will be broadened because of the gamma energy deposited in the solid-state detectors. This thermal peak broadening is identical to the alpha peak broadening discussed previously.

Once again a simple order-of-magnitude calculation can be performed to show that the measured increase in count rate can be accounted for by considering the additional threefold coincidences which occur when a gamma ray triggers a solid-state detector in coincidence with a neutron-induced coincidence between the proportional counters. The rate of accidental coincidences, N, which can occur in this way, is given by

$$N = N_S \; N_P \; \tau_{SP}$$

where N_S is the total count rate in the two solid-state detectors, N_P is the number of neutron-induced coincidences in the proportional counters, and τ_{SP} is the resolving time for coincidences between the proportional counters and the solid-state detectors. Using the measured values of N_S, N_P and τ_{SP}, the above formula yields N = 12 counts/sec at 300 r/hr and 20 counts/sec at 600 r/hr. Since the number of neutron induced threefold coincidences was measured as 8 counts/sec, the total threefold coincidence

count rate at 300 r/hr is expected to be 20 counts/sec, and at 600 r/hr it is expected to be 28 counts/sec. By integrating the 300 r/hr and 600 r/hr curves in Figure 11 and dividing by the time for the measurement, the measured total count rates are found to be 15 counts/sec at 300 r/hr and 18 counts/sec at 600 r/hr. This is regarded as satisfactory agreement. It is noted that the experimental count rates are both lower than the expected values. This difference is believed to be due to the fact that, in the experiment, a downward gain shift with increasing gamma dose rate was observed, and thus counts were lost due to an apparent cutoff near channel 8.

It is concluded, therefore, that the measurements of the thermal peak are strongly affected by the gamma interactions in the solid-state detectors. Thus, at dose rates in excess of 300 r/hr, the thermal peak is lost in the broad continuum of accidental gamma counts.

The second effect, the downward shift of peak with increasing gamma dose rate (See Figure 11) has not been satisfactorily explained. It is potentially significant that both the alpha peak shown in Figure 9 and the thermal peak shown in Figure 11 shift to lower channels. Both peaks shift by about the same number of channels as the gamma dose rate is increased from 0 to 300 r/hr. This may imply that the peak shifting is due to baseline shift in the components which "see" high count rates. The most likely candidates are the ac-coupled components, i.e., the solid-state-detector preamplifiers (fast and slow) and the linear gate.

When the fast preamplifier was used, the alpha peak shifted upward at 10 r/hr, but this trend reversed and the alpha peak shifted downward as the gamma dose rate was increased to 300 r/hr. The alpha peak shifting with the fast preamplifier (< 8 channels) was much less than with the slow preamplifier (~ 20 channels), an observation which is as yet unexplained.

In the section discussing the alpha-source measurements in high gamma fields, it was suggested that a factor of 15 or greater improvement in dose rate could be achieved by using the $Li^6(n,\alpha)T$ reaction and thinner solid-state detectors. These modifications will also result in an important improvement in the low-energy gamma background reported here. Since the Q value of the Li^6 reaction is 4.8 MeV, the thermal neutron peak will appear at a much higher energy than the gamma background and hence should be easily identified. In Figure 11 the 4.8-MeV thermal peak would appear near channel 200, where the gamma background is virtually zero even at the highest dose rates studied here.

IV. CALCULATIONS OF DETECTOR EFFICIENCY

There are two key questions affecting the utility of this spectrometer: (1) What is the efficiency of the detector at a fixed neutron energy? and (2) How does this efficiency vary with the angle between the incident neutron trajectory and the detector axis? A computer program has been written and tested to provide some answers to these questions. This section describes the basic theory of the program and the results available to date.

If a monodriectional incident flux of 1 neutron/cm^2-sec is assumed, the number of interactions per second in a differential volume element is

$$\Sigma \, d\bar{r},$$

where Σ is the macroscopic cross section (cm^{-1}) for the reaction $He^3(n,p)T$ and $d\bar{r}$ is the differential volume element. The number of protons per second due to this reaction emerging from $d\bar{r}$ in a solid angle $d\bar{\Omega}$ is

$$(\Sigma \, d\bar{r}) \quad \left(\frac{\sigma(\theta)}{\sigma}\right) \quad d\bar{\Omega}$$

where θ is the laboratory angle between the neutron direction and the proton direction and $\sigma(\theta)/\sigma$ is the angular distribution (steradian^{-1}) of the protons for this reaction. The number of counts per second recorded due to reactions occurring in $d\bar{r}$ that result in protons within $d\bar{\Omega}$ is

$$dI = P_1 \cdot P_2 \cdot \Sigma(\theta) \cdot d\bar{r} \cdot d\bar{\Omega},$$

where

$$\Sigma(\theta) = \frac{\sigma(\theta)}{\sigma} \Sigma$$

The factor P_1 is either 1 or 0 depending upon whether the proton originating at $\bar{r}$ in a direction $\bar{\Omega}$ strikes or misses one of the two solid-state detectors, and P_2 is either 1 or 0 depending upon whether the triton emitted in this same event strikes or misses the other solid-state detector. Note that the triton must interact with a different solid-state detector than the proton.

Figure 12 depicts a typical neutron reaction. The neutrons are incident from the left, parallel to the detector axis, and undergo a reaction emitting a proton and a triton. If one assumes that the point of the interaction is known and that the angle of emission of the proton is known, one can find an expression for r_2, the distance from the detector center at which the proton trajectory intersects the solid-state detector. The factor P_1 is then defined as follows:

$$P_1 = \begin{cases} 1 \text{ if } r_2 < R \\ 0 \text{ if } r_2 > R \end{cases}$$

where R is the radius of the solid-state detector

For known directions of the incoming neutron and of the outgoing proton the kinematics of the reaction can be used to calculate the outgoing triton direction, from which one can calculate r_3 - the distance from the detector center at which the triton trajectory intersects the solid-state detector. Using the kinematics, one can also determine whether the triton is headed toward the same solid-state detector as the proton or toward the other solid-state detector. Then,

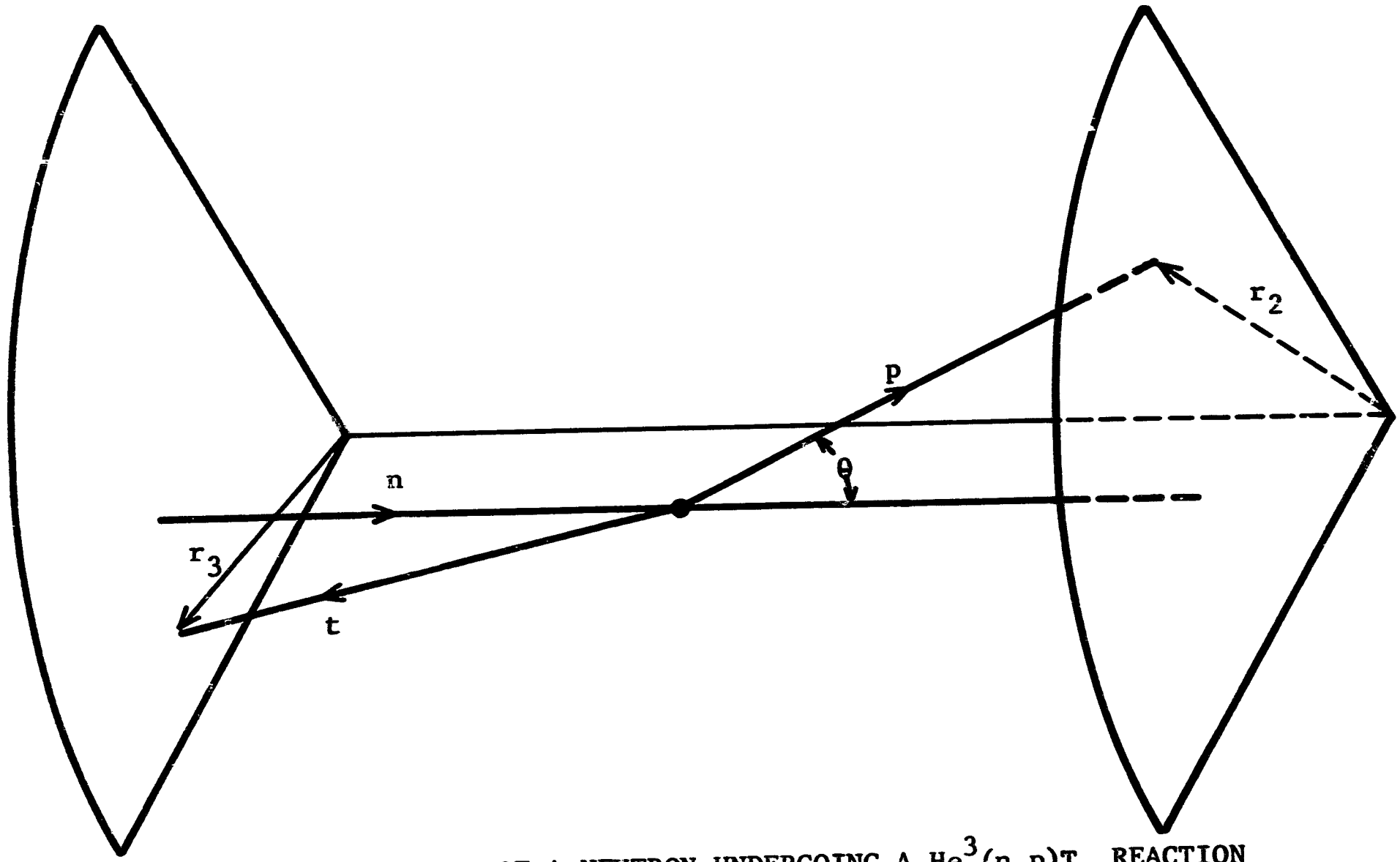

Figure 12 REPRESENTATION OF A NEUTRON UNDERGOING A $He^3(n,p)T$ REACTION

$$P_2 = \begin{cases} 1 & \text{if } r_3 < R \text{ and the proton and triton are headed toward different solid-state detectors;} \\ 2 & \text{if } r_3 > R \text{ or if the proton and triton are headed toward the same solid-state detector.} \end{cases}$$

Finally, the total number of counts per second, I, can be calculated from

$$I = \int_0^R dr \int_0^{2\pi} d\theta_n \int_0^L dz \int_0^{\pi} d\theta \int_0^{2\pi} d\theta_p \; P_1 \cdot P_2 \; \Sigma(\theta) \cdot r,$$

where (r,θ_n,z) describe the position at which the intersection took place, and (θ,θ_p) describe the direction of the emergent proton. This five-dimensional integral has been evaluated using the IITRI computer (IBM 7094) for two special cases: (1) neutrons incident parallel to the detector axis, and (2) neutrons incident perpendicular to the detector axis. In principle, all other angles of incidence can be treated but the computer running time may be excessive. The two special cases mentioned are the most interesting when monodirectional incidence is considered. If isotropic incidence or other nonmonodirectional incidence is considered, these two cases will represent an upper limit on the angular dependence of the detector response.

During the programming, careful attention was paid both to the mesh spacing and to the order in which these numerical integrations were performed. For example, the integral over θ involves the evaluation of trigonometric functions, an operation which is relatively slow on a computer (200 μsec). This numerical integral was performed last so that these functions had to be evaluated only about ten times. On the

other hand, the integral over r involves only a few algebraic manipulations which can be performed very rapidly (<10 μsec). Hence, the numerical integration over r was done at the earliest possible time in the program. For 10^5 mesh points the average running time of the computer for one neutron direction, one energy, and one detector size (cylindrical shape) was 15 seconds.

Finally, no direct measurements could be found of the angular distribution of the $He^3(n,p)T$ reaction. The cross sections used in this code were derived from the data available on the inverse reaction.* These data indicate that, at energies in the MeV range, this reaction is by no means isotropic in either the laboratory or the center-of-mass systems.

Figure 13 shows the results of a series of calculations of the isotropy of the detector response. For very low neutron energies, the angle between the proton and the triton is 180 degrees. If one assumes an isotropic cross section in the laboratory system, then the calculation for axial incidence ought to yield the same result, I_A, as the calculation for radial incidence, I_R. In the figure, the ratio I_A/I_R at $E = 10^{-7}$ MeV is plotted as a function of the ratio of radius to length, R/L. The actual results showed $|I_A - I_R| < 4$ percent for all R/L in the range (0.2 to 10).

---

*The data at 5.8 MeV were obtained from Bodgonov, Vlasov, Kalinin, Rybakov, Samoilov and Sidorov, Soviet Physics JETP (Translation) 36, No. 2, 440, August 1959. At 2.4 and 11.4 MeV the data were obtained from Goldberg, Anderson, Stovering and Wong, Phys. Rev. 122, No. 5, June 1961. Other references and intercomparisons of all available data can be found in the proceedings of the International Conference "Nuclear Forces and the Few Nucleon Problems," Vol. II, p. 583, July 1959, Pergamon Press.

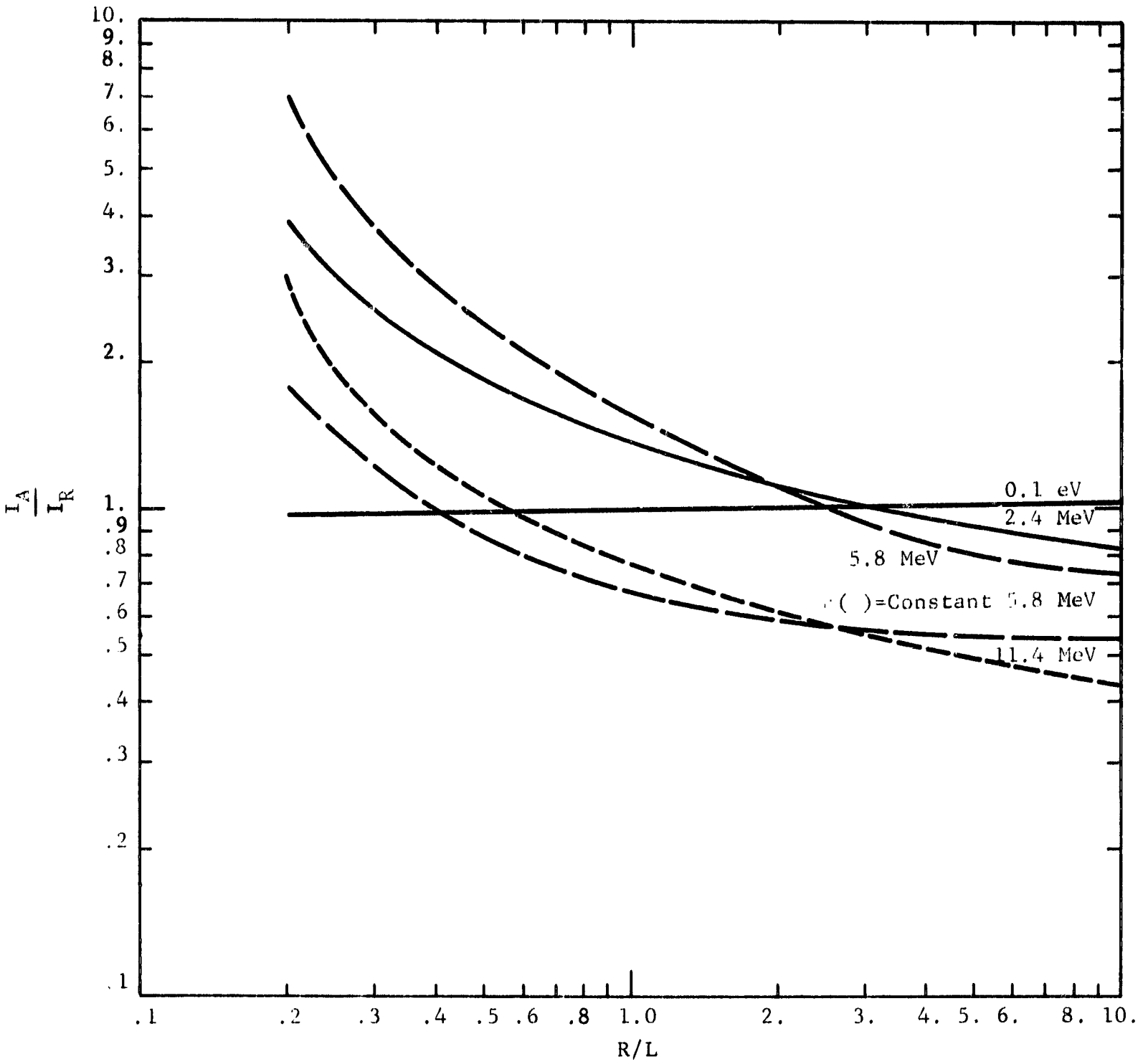

Figure 13 DETECTOR ISOTROPY AS A FUNCTION OF R/L FOR VARIOUS NEUTRON ENERGIES

This calculation lends considerable confidence that the codes are working properly and that the choice of mesh spacing is adequate for an accuracy of ± 5 percent.

At higher neutron energies the average angle between the proton and triton decreases, and the detector can no longer be expected to have an isotropic response even for an isotropic cross section. The ratio I_A/I_R is an indicator of detector isotropy. The shape of the curves of I_A/I_R as a function of R/L will be discussed below. At small R/L the detector will be more efficient for axial incidence than for radial incidence. The reason for this can be seen by noting that, in the limit $R/L \rightarrow 0$, in order to be detected, a reaction between He^3 and a radially incident neutron must produce protons and tritons emerging at right angles with respect to the incident neutrons. Since it is kinematically impossible at high neutron energies for both particles to emerge at right angles, I_R must go to zero faster than I_A; therefore, the ratio $I_A/I_R \rightarrow \infty$ as $R/L \rightarrow 0$. This feature is illustrated in Figure 13 by the sharp rise at small R/L in the curve marked E = 5.8 MeV, $\sigma(\theta)$ = constant

At large R/L, the detector will be more efficient for radial incidence. This is so because, as $R/L \rightarrow \infty$ all of the protons and tritons for radial incidence are detected. For axial incidence, only those reactions will be detected in which the protons and tritons are headed toward opposite solid-state detectors. This effect is also shown on this same curve.

If the true differential cross section (as computed from the inverse reaction) is used in the codes, the curve marked E = 5.8 MeV is obtained. Since the reaction is mostly in the forward direction at this energy, I_A is increased more than I_R and the whole curve is shifted upward from the $\sigma(\theta)$ = constant case.

From Figure 13 an optimum detector shape can be determined. Optimum shape is defined in this report as that value of R/L for which the maximum value of $\left|I_A/I_R - 1.0\right|$ for all neutron energies is the smallest. Other definitions of optimum shape are, of course, possible; in particular, the optimum shape will depend on the nature of the spectrum to be measured and on the relative importance of the various spectral regions. The highest neutron energy for which cross-sectional data were available was 11.4 MeV, and the smallest was 2.4 MeV. If one assumes that the data used represent extreme cases, one finds, from Figure 13 that the optimum R/L is about 1.4.

The current detector was designed before these calculations were performed; for it, the value of R/L is 0.31. Figure 13 shows that this detector can be expected to be highly anisotropic.

Figures 14 and 15 show the calculated absolute radial and axial efficiency (equals I/projected area) as a function of neutron energy for various ratios R/L. The He^3 gas pressure was taken as 1 atmosphere. Comparison with the $He^3(n,p)T$ reaction cross section shows that the shapes of these curves do not differ very much from the shape of the cross-section curve.

In summary, these calculations indicate that the present detector does not have an isotropic response. The degree of anisotropy depends upon the shape of the detector. For a cylindrical detector having a radius of 1.4 times the length, the anisotropy is a minimum, $\left|I_A/I_R - 1.0\right| < 0.32$. For this size detector, the efficiency in counts per unit neutron flux will be of the order of 10^{-5} to 10^{-6}. For radial incidence, the efficiency and the $He^3(n,p)T$ cross section exhibit about the same energy variation.

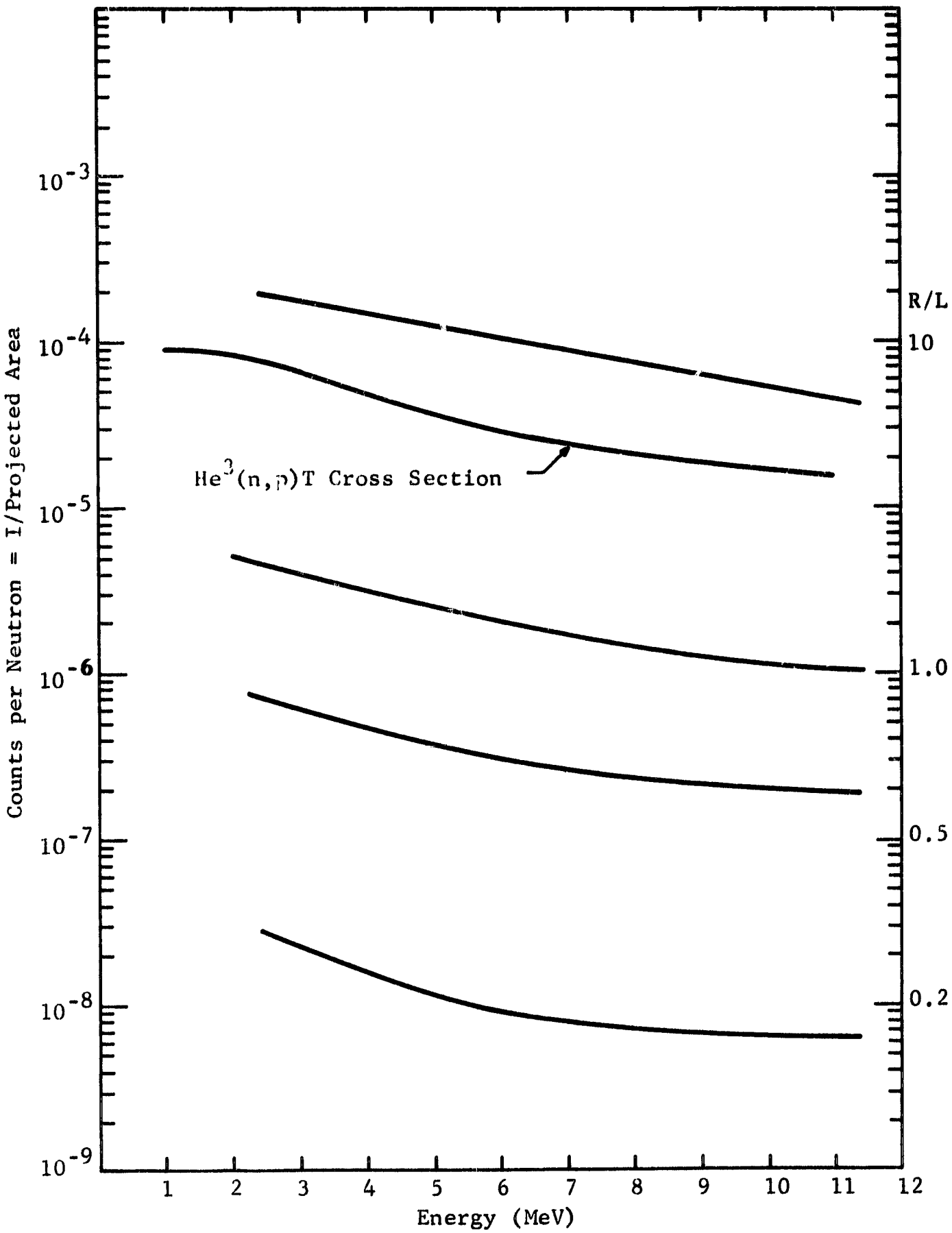

Figure 14 DETECTOR EFFICIENCY AS A FUNCTION OF ENERGY FOR VARIOUS SHAPES, RADIAL INCIDENCE

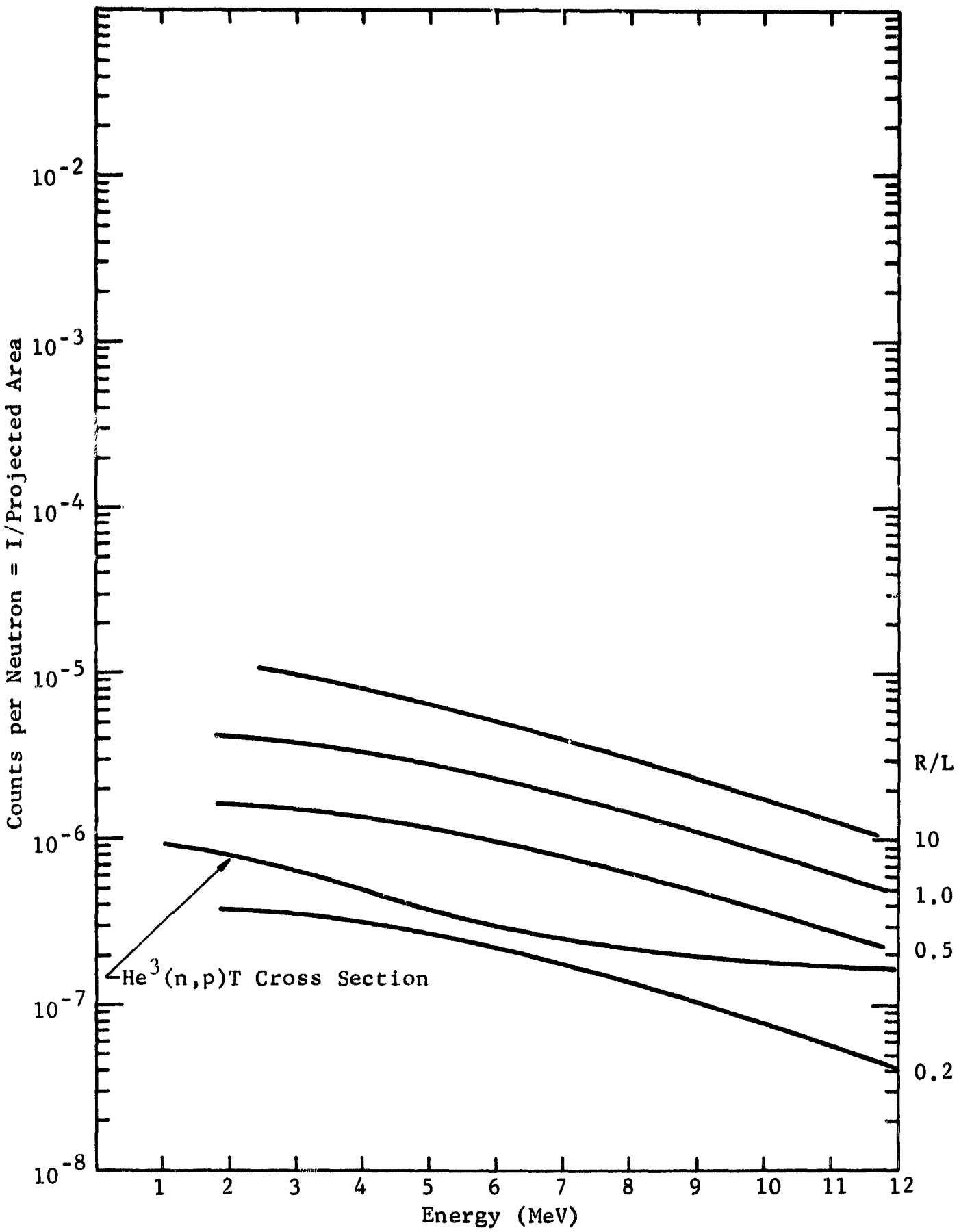

Figure 15 DETECTOR EFFICIENCY AS A FUNCTION OF ENERGY FOR VARIOUS SHAPES, AXIAL INCIDENCE

V. CONCLUSIONS

A new neutron-spectrometer system has been built and tested in preprototype form. The system has some important advantages over conventional designs, especially when performance in high gamma fields is important. While it now seems clear that the original goal of operation in gamma dose rate fields up to 10^6 r/hr is unachievable, a partially successful system has been demonstrated in gamma fields up to 300 r/hr. In order to reduce the disparity between the maximum permissible gamma dose rate and the desired dose rate, a modification of the system has been suggested and discussed. With this modification, the maximum permissible dose rate may be increased by a factor of 15 or more to a dose rate approaching 10^4 r/hr. Since the required dose rate may be lower than the original specification, the disparity may not be quite as great as is indicated by the numbers above. Furthermore, the use of external shielding against gamma radiation has not been considered thus far. If a minimal amount of lead shielding is incorporated, it is expected that this spectrometer design can make a valuable contribution for the intended application.

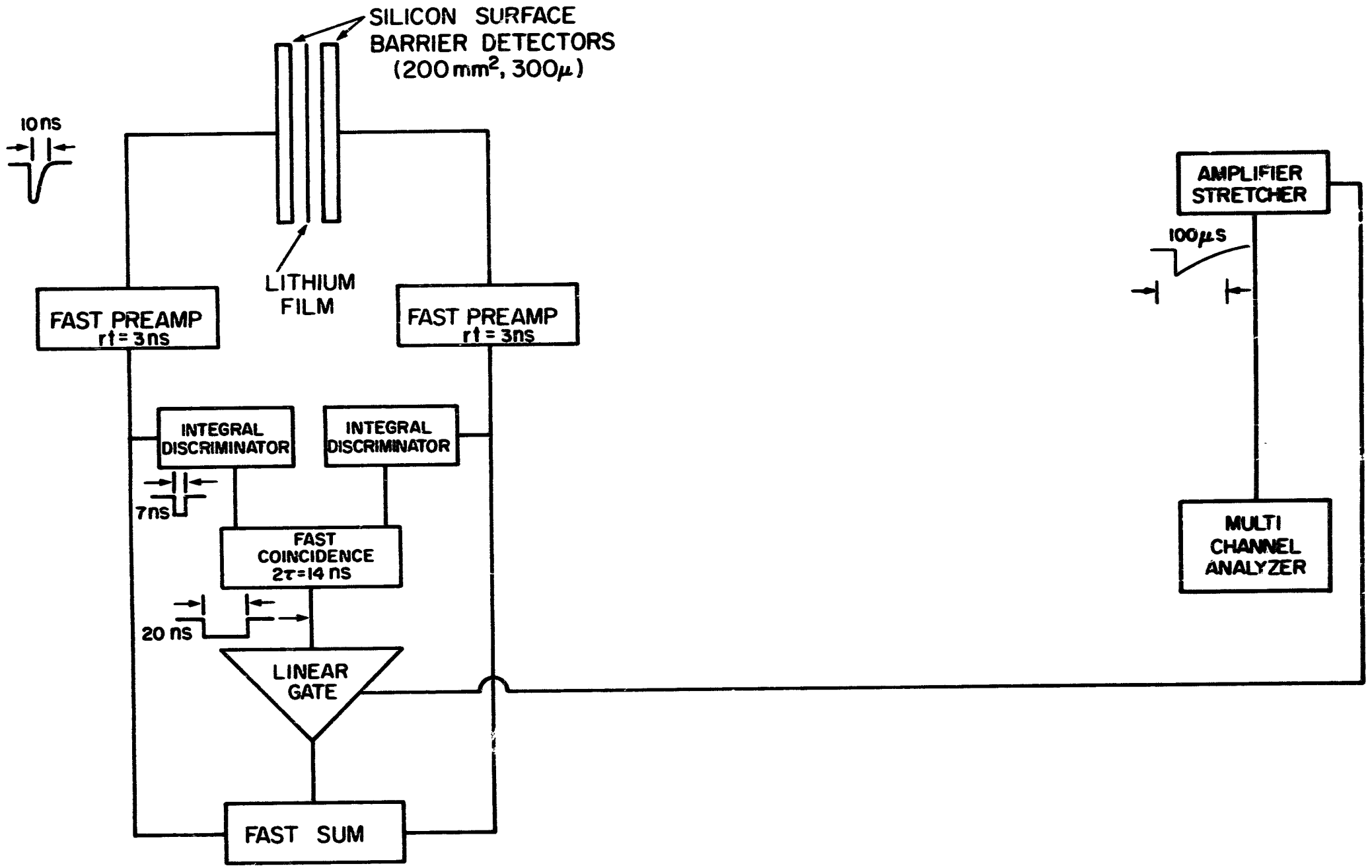

Figure 16 SCHEMATIC REPRESENTATION OF A HIGH SPEED SANDWICH SPECTROMETER, EXCLUDING PROPORTIONAL COUNTER

the suppression of the silicon reactions, it will permit measurements at neutron energies up to at least 14 MeV. This suppression is expected to be more nearly complete in this case than it was for the He^3 converter since a triton, rather than a proton, is being recognized. For the materials involved (Si, O, Al, Fe), no reactions are known which will produce a triton.

A schematic circuit diagram for the composite system is shown in Figure 17. The components added to the system in Figure 17 are for particle recognition. This recognition is accomplished using the same E·dE/dx technique and the same circuitry as in the Figure 1 system.

A notable change in the combined system is that only one proportional counter is used in the detector assembly. This simplification arises because the Li^6 converter material is in the form of a localized thin film, whereas the He^3 converter material was a gas. The extended volume source dictated by the gaseous converter required that the active volume be divided into two proportional counters to ensure that the desired reaction products could traverse at least one complete proportional counter.

The program associated with the development of the system based on a Li^6 sandwich detector incorporating particle recognition, is divisible into two distinguishable phases having well defined goals. The first pahse is limited to a thorough evaluation of the maximum permissible gamma dose rate. If, at this maximum, the thermal peak resolution is satisfactory, i.e., less than 0.5 MeV, then the second phase will be initiated. The objective of this second task is to determine the performance of the particle recognition circuitry, and, when this has been accomplished, to carefully evaluate the complete spectrometer. To accomplish these

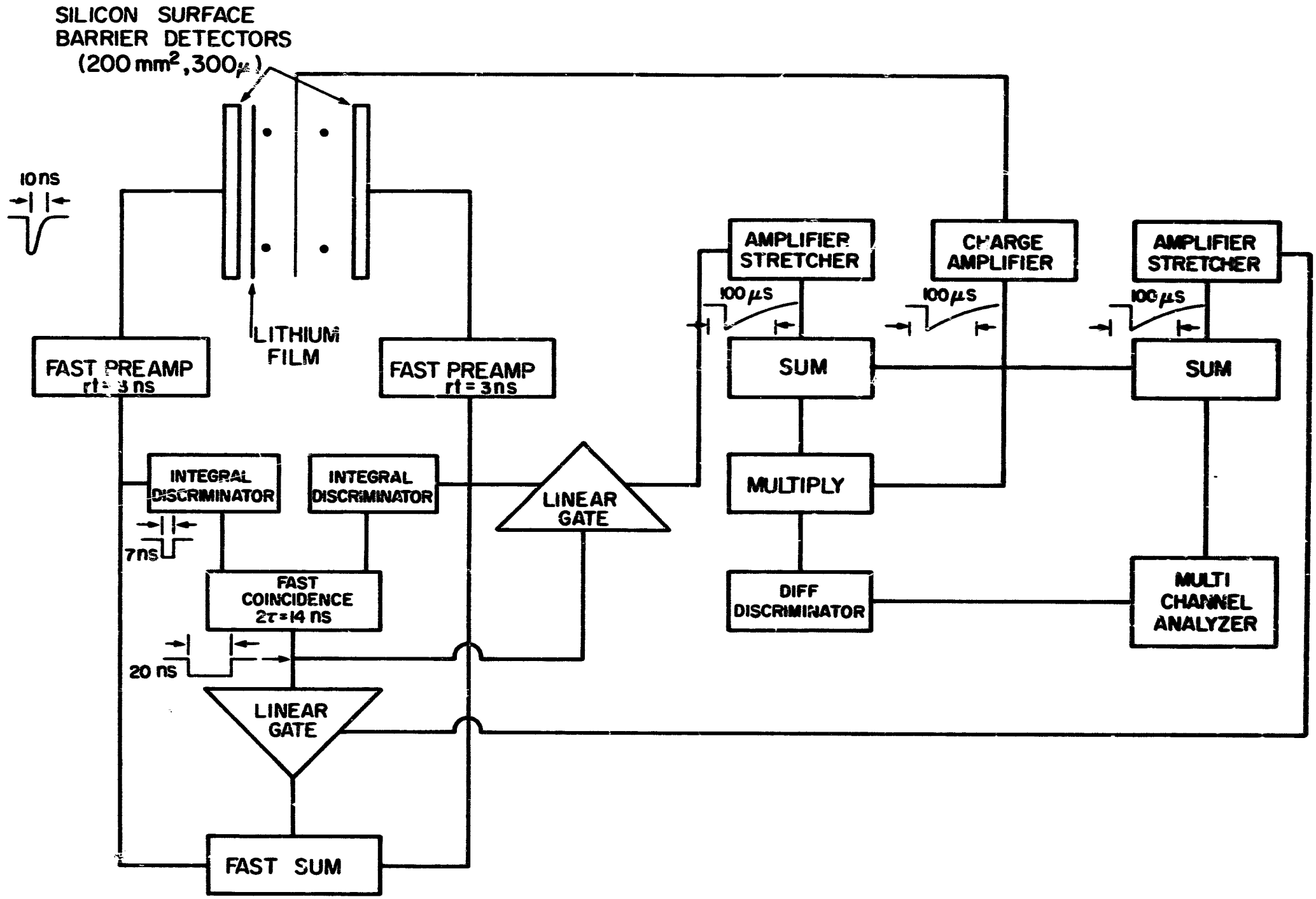

Figure 17 SCHEMATIC REPRESENTATION OF A HIGH SPEED SANDWICH SPECTROMETER, INCLUDING PROPORTIONAL COUNTER

objectives, the spectrometer is exposed to 14-MeV neutrons and measurements made of the factor by which the silicon reactions are rejected by the particle recognition circuitry. Measurements in a thermal reactor spectrum are desirable also to determine the importance of silicon reactions in the intended application.

It is important to note that there is a high probability of achieving these objectives because of the excellent foundation of experience and knowledge resulting from the work discussed in this report, the relative simplicity of the electronic ensemble, the evidence provided by Nygaard, and the division of the program into two separate tasks. The removal of the proportional counters from the fast-coincidence requirement is expected to be an additional operational simplification which will permit a more rapid identification of the problem areas.

VI. RECOMMENDATIONS

It is recommended that further testing be performed on this type of spectrometer system to increase the maximum permissible dose rate and to simplify the electronic circuitry. Specifically, it is recommended that a sandwich spectrometer be tested using Li^6 as the converter and incorporating a proportional counter to achieve particle recognition.

Nygaard[4] has shown that $Li^6(n, \alpha)T$ spectrometers of the solid-state sandwich type can be operated with 200-keV resolution in gamma fields greater than 10^4 r/hr without any observed gamma pileup effects. He achieved this remarkable objective by using very high speed electronics and short gate widths. His system has not received further attention because the useful energy range is limited to below 2 MeV due to neutron reactions in the silicon. This point is discussed below.

The recommended research program will attempt to reproduce Nygaard's result and to determine the factors limiting the gamma dose rate in a system similar to Nygaard's. The schematic circuit diagram of such a system is shown in Figure 16. The basic simplicity of this system makes the carrying out of such a program relatively straightforward.

This system is not sufficient for the intended application because it has no provision for the elimination of interfering reactions occurring in the silicon. The IITRI technique of incorporating a proportional counter in the sandwich spectrometer will remove this limitation. Since this upgrading of the original system can be accomplished without a major revision of the diagram shown in Figure 16, the composite system will retain the excellent count rate capabilities observed by Nygaard. In addition, because of

REFERENCES

1. R. B. Miller, A Fast Neutron Spectrometer of Advanced Design, Final Report IITRI-A6135, IIT Research Institute, Chicago, Illinois, April 1966.

2. P. C. Rogers, R. L. Crawford, and J. W. Teeves, "Stable Linear Pulse-Summing Circuit," Review of Scientific Instruments, Vol. 36, p. 857 (1965).

3. N. Spielberg, "Effect of Anode Material on Intensity Dependent Shifts in Proportional Counter Pulse Height Distributions," Review of Scientific Instruments, Vol. 38, p. 291 (1967).

4. K. Nygaard, "A Fast, Low Noise Amplifier Designed for Use with He^3 and/or Li^6 Solid State Detectors Operating in Reactor Environments," Nuclear Electronics, p. 693, ENEA AB Atomenergi, Sweden (1963).